Nano Today 28 (2019) 100773

Contents lists available at ScienceDirect

Nano Today

journal homepage: www.elsevier.com/locate/nanotoday

Review

Intrinsic chemistry and design principle of ultrasound-responsive nanomedicine

Xinwu Cui [a], Xiaoxia Han [d], Luodan Yu [c], Bo Zhang [b,*], Yu Chen [c,*]

[a] Department of Medical Ultrasound, Tongji Hospital, Tongji Medical College, Huazhong University of Science and Technology, Wuhan, 430030, PR China
[b] Department of Ultrasound in Medicine, Shanghai East Hospital, Tongji University School of Medicine, Shanghai, 200120, PR China
[c] State Key Lab. of High Performance Ceramics and Superfine Microstructure, Shanghai Institute of Ceramics, Chinese Academy of Sciences, Shanghai, 200050, PR China
[d] Department of Medical Ultrasound, Shanghai General Hospital, Shanghai Jiaotong University School of Medicine, Shanghai, 200080, PR China

ARTICLE INFO

Article history:
Received 5 May 2019
Received in revised form 16 August 2019
Accepted 26 August 2019
Available online 9 September 2019

Keywords:
Ultrasound imaging
Ultrasound therapy
Nanomedicine
Chemistry
Nanoparticles

ABSTRACT

Chemistry has long been playing its specific role in ultrasound-responsive theranostic biomedicine in the form of microbubbles, which clinically provide the dynamic detection of macro and microvasculature by continuous expanding and contracting under the alternating ultrasound pressure. However, microbubbles' large particle size severely hinders their efficiency in ultrasound-triggered diseases theranostics as they only transport within the blood vessels. Fortunately, the scientific community recently seeks solving strategies from the advances of chemistry and nanomedicine by rationally designing and fabricating versatile intelligent and multifunctional ultrasound-responsive nanosystems/nanoplatforms to solve the critical issues of traditional microbubbles and routine nanosystems, which is herein classified as "ultrasound-responsive nanomedicine". This review discusses and clarifies the intrinsic chemistry (*e.g.*, material chemistry, surface chemistry, physiochemistry and biochemistry) and design principle of versatile nanosystems/nanoplatforms with unique ultrasound response not only for diagnostic bioimaging (single and/or multi-modality ultrasound imaging), but also for multiple ultrasound-triggered therapeutic applications. Based on the unique ultrasound features of high tissue-penetrating capability, non-invasiveness, easy accessibility and relatively mature apparatus, this review finally elucidates the unresolved critical issues/challenges and future clinical-translation potentials of this intriguing "ultrasound-responsive nanomedicine".

Contents

* Corresponding authors.
E-mail addresses: zhangbo2016@tongji.edu.cn (B. Zhang), chenyu@mail.sic.ac.cn (Y. Chen).

https://doi.org/10.1016/j.nantod.2019.100773
1748-0132/

Introduction

Nanomedicine has been developed as the alternative but highly efficient strategy for solving some critical issues of disease diagnosis and therapy in clinic [1–6]. Especially, the rational design of intelligent nanomedicine with unique responsive characteristics to either external physical irradiation or internal disease-microenvironment triggering has attracted broad research interest because of the underlying high controllability and efficiency during the theranostic process on various diseases [7–9]. The exogenous energy input for theranostic nanomedicine is highly promising where diverse triggering sources have been employed, including light [10,11], ultrasound (US) [12,13], magnetic field [14,15], electric field [16], *etc*. It has been thoroughly explored that light can be used for either optical biological imaging or therapeutic use such as photothermal therapy (PTT) or photodynamic therapy (PDT) [17,18]. Although traditional light-triggered theranostic nanomedicine is featured with non-invasiveness, the optical imaging or therapy encounters the limitation of its scattering in tissue that hinders the tissue imaging/therapy at depths no more than 1 mm [19,20]. Comparatively, US is featured with much lower scattering in tissue with the imaging resolution of the order of 100 μm and depth of more than several centimeters [21,22]. Integrated with the characteristics of non-invasiveness, high biosafety and low cost, US-based imaging or therapy has been extensively used in clinic currently [23–25].

Gas-involved microbubbles (MBs) have been clinically used in contrast-enhanced diagnostic US imaging based on their cost-effective and biocompatible features, as well as their intriguing scattering acoustic property and specific nonlinear interaction with incident US, which significantly improve the signal-to-noise ratios of ultrasonography [26–28]. In addition, MBs have recently been employed for the delivery of therapeutic agents for ultrasonography-guided therapeutic applications [29,30]. However, these MBs have the limitations of large particle size in the range of several micrometers, making them only produce contrast-enhanced US imaging within the vasculature based on their short circulation lifetime within and poor extravasation from the blood vessel [31]. In addition, the easy gas diffusion and potential biological clearance of MBs also cause their short *in vivo* circulation duration [28].

Owing to the specific drawback that MBs only produce contrast-enhanced US imaging within the vasculature because of their micrometer size, some small-sized nanoagents have recently been constructed as these MBs alternatives. It has been found that these versatile nanoformulations and nanoplatforms have also been used for US-based therapeutic applications, which has got fast progress very recently. Typically, these nanosystems are rationally designed with unique US response for either diagnosis or therapy of diseases, which are mainly based on their intrinsic physiochemical properties. For instance, some US-responsive nanoparticles could produce reactive oxygen species (ROS) upon US irradiation, which is typically termed as sonodynamic therapy (SDT) in comparison to traditional light-triggered PDT [32–35]. The corresponding nanosystems are defined as nanosonosensitizers [36,37]. To improve the thermal-ablation efficacy of high intensity-focused US (HIFU), some nanoagents were designed as the synergistic agents for changing the acoustic microenvironment of tumor and subsequently enhancing the HIFU ablation outcome [38–45]. The unique biological effects of US could also be used for rational design of US-responsive nanoplatforms for achieving some specific theranostic purposes, such as the well-known assistance on blood brain barrier (BBB) crossing of nanoparticles for the treatment of diseases in brain and enhancing the extravasation of nanoparticles out of the blood vessels for tumor-tissue accumulation.

Chemistry plays the critical role on the design of these US-responsive nanomedicines. For instance, the principle of material chemistry and nano-synthetic chemistry guarantees the fabrication of US-responsive nanoparticles with desirable crucial structural and compositional parameters. The versatile surface chemistry of these US-responsive nanosystems can be chosen for surface engineering such as PEGylation for improving the blood-circulation duration and targeting conjugation for enhancing the accumulation into the lesion tissues. Importantly, the unique physiochemical property of these US-responsive nanoplatforms and biological chemistry of US can be employed for achieving high theranostic efficacy on disease treatment. Based on the rapid development of this intriguing US-based theranostic nanomedicine, this review summarizes and discusses the underlying intrinsic chemistry of US-responsive nanomedicine, including material chemistry, surface chemistry, physiochemistry and biochemistry (Fig. 1). Especially, the paradigms of nanomedicines-enhanced disease theranostics by US are discussed in detail to reveal the design principle of US-responsive nanoplatforms from the viewpoint of chemistry, including US imaging (*e.g.*, single modality imaging and multi-modality imaging), US therapy (*e.g.*, SDT, HIFU ablation, drug release, gene therapy, crossing BBB, synergistic therapy, *etc*.) and US theranostics (*e.g.*, US-imaging guidance, US-imaging monitoring and other imaging modality-enabled US theranostics). By presenting the current challenges on the further clinical translation of these US-responsive nanomedicines, this review finally outlooks the future development and prospect of this unique interdisciplinary field regarding material science, chemistry, biomedicine and physical US.

Materials chemistry on the design and fabrication of US-responsive nanomedicine

The successful fabrication of intriguing US-responsive nanosystems/nanoplatforms with pre-designed composition, nanostructure and functionality is the premise for US-triggered theranostic applications, which is typically based on the underlying material chemistry and nano-synthetic chemistry [46]. The currently explored US-responsive nanoparticles are either organic, inorganic or even organic-inorganic hybrid nanosystems (Table 1). Therefore, their synthetic methodologies are significantly different from each other, which means that the underlying material chemistry also varies among these versatile US-responsive nanosystems. For instance, perfluorocarbon (PFC) is generally used for the construction of phase-changeable nanoparticles for US theranostics and porphyrin-based nanomedicine is usually employed for sonodynamic tumor therapy. Especially, materials chemistry herein refers to the underlying chemistry of the rational construction of various US-responsive nanoparticles with different nanostructures and some key parameters such as particle size, dispersity, morphology, porosity, *etc*.

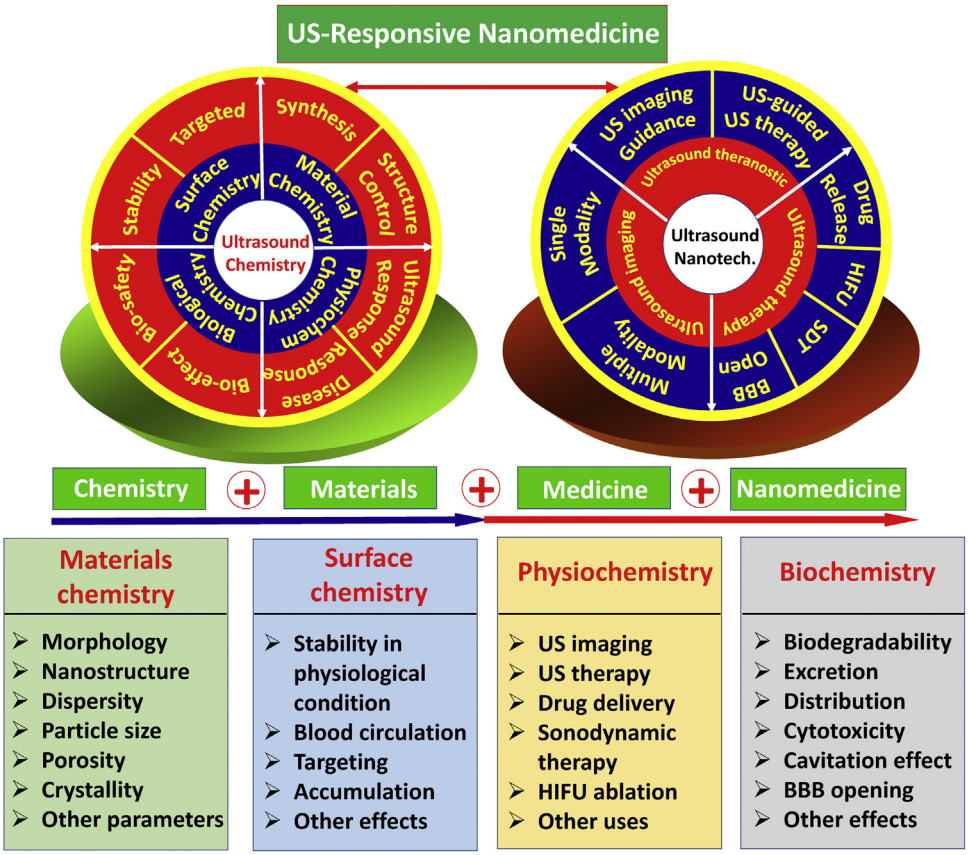

Fig. 1. Summative scheme of the intrinsic chemistry related to US-responsive nanomedicine (*e.g.*, material chemistry, surface chemistry, physiochemistry and biological chemistry), and the nanotechnology-enabled US-based versatile biomedical applications, including US imaging (*e.g.*, single modality imaging and/or multi-modality imaging), US therapy (*e.g.*, SDT, HIFU ablation, drug release, gene therapy, crossing BBB, synergistic therapy, *etc.*) and US theranostics (*e.g.*, US-imaging guidance, US-imaging monitoring and other imaging modality-enabled US theranostics). The relationship between chemistry and US-responsive nanomedicine is also shown in the scheme.

Table 1
Summative table of the comparison between US-responsive organic nanosystem and inorganic nanosystem.

Comparison	US-responsive organic nanosystem	US-responsive inorganic nanosystem
Classification	Nanosystem with pure organic components and compositions.	Nanosystem with pure inorganic components and compositions.
Types	Liposome, PLGA, emulsion, nanobubbles, nanoscale microorganism, nanodroplets, other polymer nanoparticles, *etc.*	Silica-based nanoparticles such as mesoporous silica, semiconductors such as TiO_2, Au, Fe_3O_4, $CaCO_3$, MnO_x, graphene oxide, HMSNs, *etc.*
Advantages	High biocompatibility, easy biodegradation and excretion, high US response and easy fabrication.	Easy modulation of monodispersity, crucial structure/composition and multifunctionality such as photonic, acoustic, magnetic and catalytic property, and high stability.
Disadvantages	Single functionality, difficulty in modulating functionality and structure/morphology/composition, low stability, *etc.*	Low biodegradability, unclear biocompatibility and biosafety, low US response, *etc.*

The organic nanoparticles are typically synthesized by self-assembly process where the precise determination of reactant concentration and synthetic condition could control the particle size, morphology and surface chemical status of these nanosystems. Especially, some US-responsive drug molecules were concurrently encapsulated into these organic nanoparticles during the synthetic process such as the chemotherapeutic drugs or sonosensitizers. Some liquid media such as phase-changeable PFC molecules were encapsulated into organic nanoparticles, which were further vaporized into gaseous MBs for contrast-enhanced US imaging or synergistic US therapy. The key particle size of these nanodroplets determines the vaporization temperature, which was facilely controlled by the synthetic procedure and adopted parameters. Especially, the particle size of these organic nanoparticles influences the tumor-accumulation amount and therefore determines the final theranostic efficacy and outcome. The organic nanosystems are typically featured with easy biodegradation and high biocompatibility, but their functionality to US response is relatively difficult to be controlled.

Inorganic nanoparticles are featured with their intrinsic US-responsive functionality where the synthetic procedure also substaintially determines their theranostic performance. For instance, the typical inorganic TiO_2 nanoparticles as nanosonosensitizers exhibit low US response to produce ROS because of easy re-combination of US-excited electrons (e^-) and holes (h^+) [47]. The further creation of oxygen defects on the surface of TiO_2 nanoparticles (black TiO_2) enhanced separation efficiency of US-excited electrons and holes [48]. Especially, the integration of TiO_2 with conductive graphene oxide achieved the similar enhancement effect [49]. The construction of hollow nanostructure in mesoporous silica nanoparticles (MSNs) by hard-templating method could load hydrophobic perfluorohexane (PFH) molecules with large amount for HIFU-triggered

liquid-gas phase transition and subsequently improving the HIFU ablation efficacy, where the hollow nanostructure was necessary for the high loading of guest molecules, especially for hydrophobic agents [13,50–52]. The rational creation of US-responsive "gatekeepers" in drug-delivery nanosystems realized US-controlled drug release by breaking up these "gatekeepers" [53,54], and the integration of functional contrast agents into one composite nanosystem achieved diagnostic imaging-guided US therapies [13]. Typically, inorganic nanoparticles have their intrinsic physiochemical property such as catalytic activity with the response to external triggers including light, US and magnetic-field activation, endowing them with multifunctionalities for versatile biomedical applications. However, inorganic nanoparticles typically suffer from the low biodegradability and unclear biological effects and biosafety, significantly hindering their further clinical translation.

Surface chemistry of US-responsive nanomedicine

Generally, the as-synthesized nanoparticles by various synthetic chemistries cannot be directly used for disease theranostics, especially for most inorganic nanosystems. The adequate surface engineering can improve the physiological stability of these nanoparticles and prolong their blood-circulation duration. Especially, the artificial surface-targeting modification can enhance the accumulation amounts of nanoparticles into the lesion tissue, which is effective to achieve the desirable theranostic outcome with minimized administration amounts of nanoparticles. This common principle is also applicable to US-responsive nanomedicines where the adequate surface engineering of these nanoparticles is highly important and necessary. Therefore, surface chemistry herein refers to the surface engineering/modification of these US-responsive nanoparticles, which is of high significance for guaranteeing *in vivo* biomedical applications of these nanoparticles.

For nanoparticle-enabled US theranostics, 29 amino-acid brain-targeting RVG peptide was conjugated onto the surface of protoporphyrin IX-loaded nanoporous carbon-based nanoparticles for effective BBB crossing by trussing up the specific *n*-acetylcholine receptors in the brain parenchyma cells and BBB, which enhanced the therapeutic efficacy of nanosonosensitizer-enabled treatment of Alzheimer's disease (AD) [55]. The surface of mesoporous organosilica nanoparticles as the organic sonosensitizer carrier was PEGylated for guaranteeing high stability and dispersity in physiological solution and even blood vessel [56]. The surface of inorganic titanium dioxide (TiO_2) nanoparticles was conjugated with avidin protein for discriminating cancerous cells from healthy cells, and subsequently induced the death of MCF-7 cancer cells [57]. We recently anchored RGD (Arg-Gly-Asp) peptide onto the surface of mesoporous nanosonosensitizers (PpIX@HMONs-MnO_x-RGD) for targeted accumulation of these nanosonosensitizers into tumor tissue of U87 tumor xenograft on nude mice for enhanced SDT efficacy [58]. The conjugation of affibody molecules onto the surface of nanobubbles achieved high specific affinity to human epidermal growth factor receptor type 2 (HER2)-overexpressed tumors with contrast-enhanced US imaging performance, showing high molecular US imaging potential [59]. In addition, the cell membrane such as red blood cell membranes was coated onto the surface of nanoparticles or nano-contrast agents for prolonging the blood-circulation durations [60,61]. From these surface-engineering paradigms, it is strongly suggested that the surface chemistry should be taken into full consideration when the US-responsive nanomedicines are designed for specific disease theranostics.

Physiochemical property of nanomedicines for US theranostics

The theranostic performance of US-responsive nanomedicines is strongly dependent on the physiochemical property of these versatile nanosystems. For instance, the liquid-gas phase-changeable behaviour of nanosized contrast agents can be used for contrast-enhanced US imaging with comparable performance to traditional MBs while overcoming their particle limitation because of the post-enlarged size and post-generated MBs. Some organic micelles encapsulating near-infrared dyes or inorganic nanoparticles have been developed as the contrast agents for photoacoustic (PA) imaging [62–65]. The semiconductor nature of TiO_2 nanoparticles can be excited for SDT. The US-responsive break-up nature of drug-delivery nanosystems is effective to achieve intelligent and controllable drug release. Therefore, the rational design of endowed physiochemical property of US-responsive nanoplatforms is the mostly explored aspect in this field, which is clarified in detail in the following sections.

Phase-changeable property of nanomedicines for US imaging

The rational design of nanosized contrast agents for US imaging should solve the critical issue of minimal acoustic contrast because of the small nanoparticulate size, which is typically produced through Rayleigh scattering of sound [66]. The effective ultrasonography requires the large enough size generally in the range of several micrometers. Traditional MBs satisfy the effective ultrasonography because of their large-enough particle size and elastic shell, which can strengthen the resonance reflection at the diagnostic US frequency. However, their large particle size in the range of several micrometers cannot infiltrate the leaky vasculature of tumors because of the presence of size limitation of less than 700–800 nm, the well-known endothelial gap junction size range in tumor vasculature [31,67,68]. It is therefore still a critical challenge to combine the advantages of nanosized contrast agents with long blood-circulation duration and enhanced permeability and retention (EPR) effect-induced tumor accumulation and micrometer-sized MBs with effective US responsibility.

The past five years has witnessed the significant progress of developing strategies for solving this critical size issue. The mostly explored methodology is the elaborate design of phase-changeable nanosystems, which can easily circulate within the blood vessel and efficiently accumulate into tumor tissue. The subsequent phase change of these nanosystems produces large micrometer-sized MBs for desirable ultrasonography. This phase-changing procedure is initiated by either tumor microenvironment (*e.g.*, pH, H_2O_2 overexpression, reducing condition, specific enzyme *etc.*) or external energy put (*e.g*, light, US, magnetic field, radiofrequency, *etc.*). The other methodology is based on *in-situ* transformation of MBs into small nanosized bubbles by varied triggers, which then penetrate the tumor for some specific theranostic purposes [69]. Especially, such a phase-changeable process has been further explored for achieving ultrasonography-guided therapeutic applications, including alleviating tumor hypoxia [70,71], chemotherapy [72], PDT [73,74] and even some synergistic-therapeutic modalities [38,75,76]. All these intelligent nanosystems and their corresponding outstanding ultrasonographic properties are based on their unique and intrinsic physiochemical properties, which are clarified in detail in the following sub-section based on some representative paradigms.

Rational integration of US-imaging modality with other imaging modalities towards multi-modality imaging can combine the unique feature of individual imaging modality, providing supplementary diagnostic-imaging information for diseases. On this

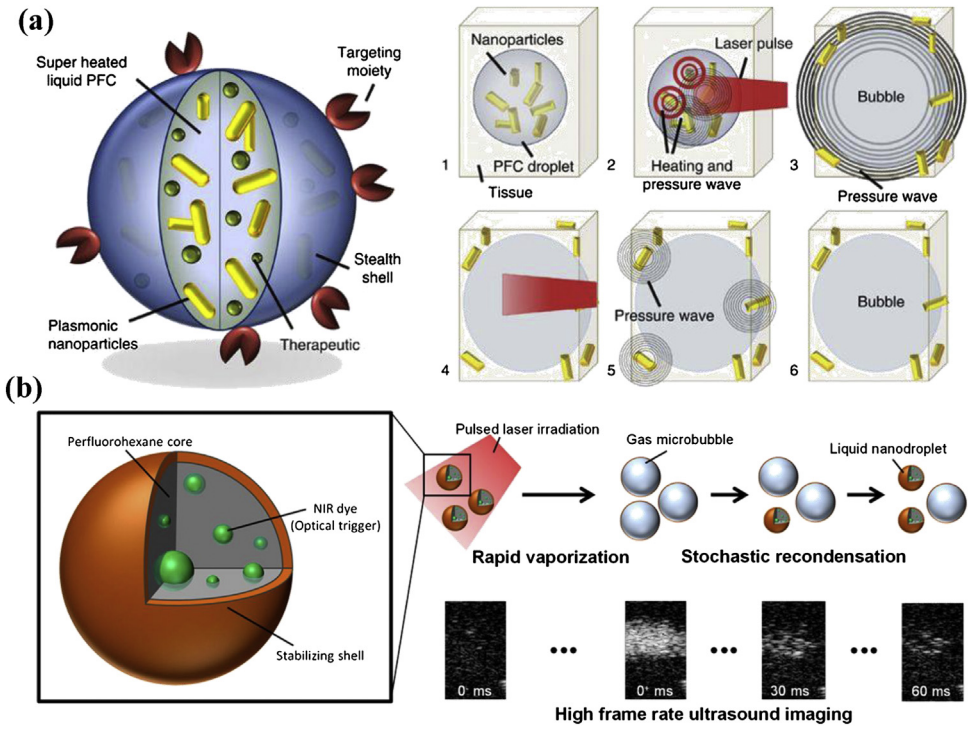

Fig. 2. (a) Schematic illustration of microstructure of as-designed PAnDs nanoparticles and their specific functionality as dual contrast agents for both PA imaging and ultrasonography, including remote activation of PAnDs, vaporization of PAnDs and thermal expansion. The post-produced PFC gaseous MBs acted as the contrast agents for US imaging based on the acoustic impedance mismatch between PFC gas MBs and the surrounding tissue microenvironment.

Adapted from Ref. [77] with permission of Nature Publishing Group, Copyright 2012. (b) Schematic illustration of the composition of LANDs with a PFH core, the encapsulated optical trigger such as NIR dye and a stabilizing shell. These LANDs were transformed from liquid to gas status by activation of a pulsed laser irradiation, which reflected acoustic waves to enhance the contrast of US imaging. The US imaging was enabled by immediate laser triggering, but such an enhancement was faded 30 and 60 ms after the laser pulse, showing the blinking phenomenon of LANDs for US imaging. Adapted from Ref. [78] with permission of American Chemical Society, Copyright 2016.

ground, the construction of multifunctional nanosized contrast agents for multi-modality imaging is of high significance. Both photoacoustic (PA) imaging and US imaging are related to US detection, which individually provides supplementary imaging information for disease diagnosis. On this ground, PA nanodroplets (PAnDs) were designed for optically activated contrast-enhanced PA imaging and ultrasonography [77]. The droplet of liquid PFC (perfluoropentane with the boiling point of 27 °C) specially capped with plasmonic Au nanorods were encapsulated into a bovine serum albumin (BSA) shell (Fig. 2a). The presence of BSA shell not only substaintially lowered the surface tension of nanodroplets for avoiding the coalescence, but also prevented the potential premature vaporization of loaded PFC based on the elevated boiling point after nanoencapsulation. Upon external laser activation, the liquid PFC core was converted from liquid to gas, which generated PFC gaseous MBs. Two effects were produced during the liquid-to-gas phase transition. On one hand, the strong PA signal was generated based on the vaporization and prolonged thermal expansion, which was effective in enhancing PA imaging. On the other hand, the produced PFC gaseous MBs increased the acoustic impedance mismatch between the gaseous MBs and surrounding tissue microenvironment, producing contrast-enhance ultrasonography effect. This dual contrast-enhancing effect in PA and US imaging was demonstrated in an *in vivo* murine model for imaging highly optically scattering and absorbing tissues [77].

In addition, laser-activated nanodroplets (LANDs) were designed with a perfluorohexane (PFH) core with the boiling point of 56 °C, an encapsulated NIR dye (Epolight 3072) as the photo-absorber for photothermal conversion and triggering, and a stabilizing shell of lipid, protein or polymer (Fig. 2b) [78]. The localized photothermal conversion by irradiation of a pulsed laser vaporized the PFH core to produce transient PFH gaseous MBs with the lifetime of tens to hundreds of milliseconds. The "on" states of MBs generation enhanced the contrast of ultrasonography and the "off" state of re-condensation to the liquid nanodroplet faded the contrast enhancement (Fig. 2b). This "blinking" phenomenon was further used to localize *in vivo* position of delivered LAND positions, which exhibited an intriguing order of magnitude improvement as compared to conventional US imaging, potentially providing a new strategy for high-resolution *in vivo* ultrasonography [78]. In addition to the phase-changeable property of nanosized PFH for contrast-enhanced US imaging, it could act as the O_2 reservoir for delivering O_2 into tumor tissue to relief the tumor hypoxia and enhance Ce6-based PDT efficiency [74].

In addition to the mostly explored PFC nanodroplets for phase change-enhanced ultrasonography, rational design and choice of nanocarriers and phase-changeable substance could also achieve the similar or enhance better theranostic outcomes. A supramolecular hybrid multifunctional material system was constructed by loading a pillar [6]arene-based host-guest complex onto the surface of 2D graphene oxide (GO) for contrast-enhanced US and PA dual-modality imaging (Fig. 3) [79]. Especially, the photothermal effect of these multifunctional agents transformed NIR light into heat, which triggered the decomposition of loaded bicarbonate counterions for generation of CO_2 nanobubbles. These post-generated CO_2 nanobubbles significantly enhanced both US and PA contrast, providing a unique paradigm of employing host-guest chemistry for the construction of supramolecular hybrid nanosystem in US-based multi-modality imaging. The delivery of catalase by zeolite nanocapsules directly catalyzed the decomposition of tumor-overexpressed H_2O_2 into oxygen MBs, which

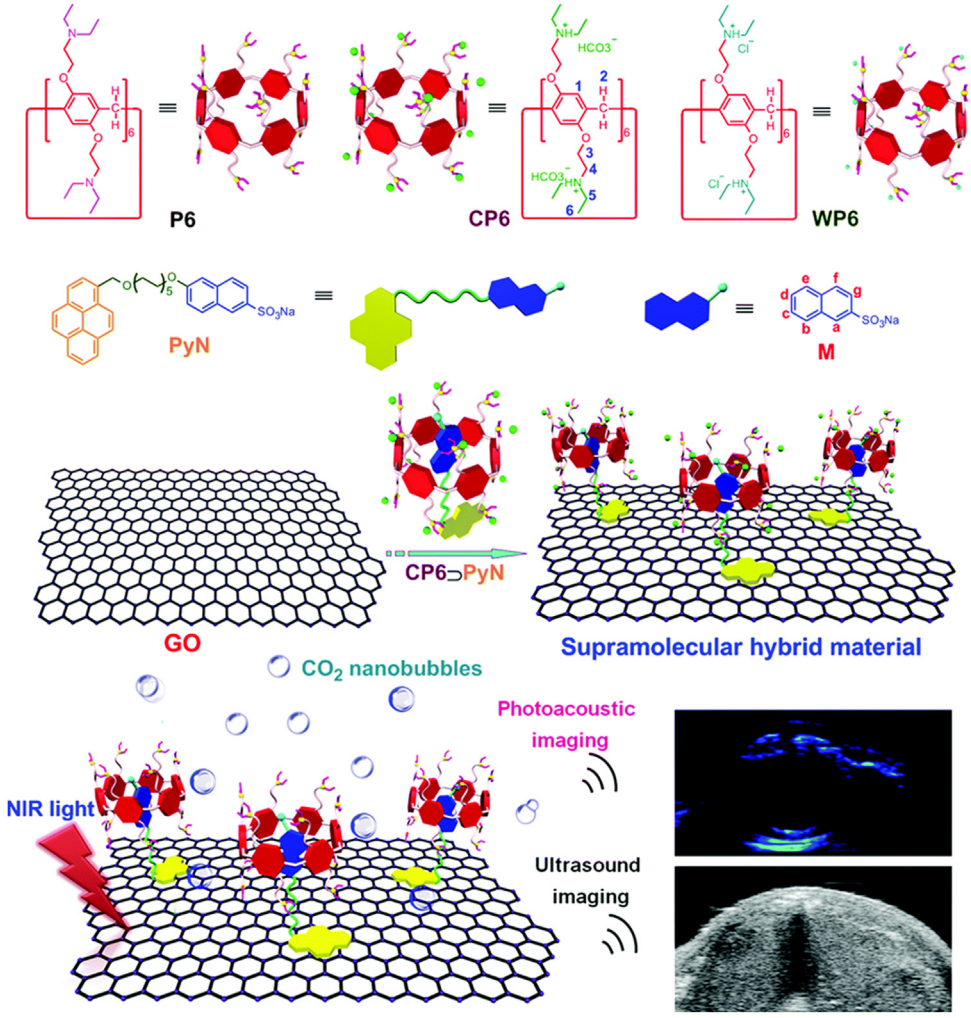

Fig. 3. The scheme of the fabrication of a supramolecular hybrid system based on the efficient loading of a pillar[6]arene-based host-guest complex onto the surface of graphene oxide (GO), and its unique functionality for NIR-triggered generation of CO_2 MBs, enhancing the contrast of both ultrasonography and PA imaging. Adapted from Ref. [79] with permission of Royal Society of Chemistry, Copyright 2018.

subsequently enhanced the intratumoral US contrast and modulated the tumor hypoxia to improve the PDT efficiency [71].

The aforementioned phase-changeable nanosystems for contrast-enhanced ultrasonography are mainly based on gaseous PFC, O_2 or CO_2 MBs or nanobubbles, the gases without obvious therapeutic functionality. Recently, hydrogen sulfide (H_2S) gas-based MBs were introduced for both ultrasonography and synergistic cancer therapy originating from anethole dithiolethione (ADT), a H_2S pro-drug (Fig. 4) [80]. In detail, ADT-loaded magnetic nanoliposome (designated as AML) with the particle size of about 200 nm were initially fabricated. The nanosize of these AMLs enabled the targeted accumulation into tumor as assisted by an external magnetic field. The delivery of ADT as the H_2S donors produced H_2S bubbles by an enzymatic trigger, which achieved the transformation of nanoliposomes to micro-sized H_2S bubbles for contrast-enhanced US imaging. Especially, the post-produced H_2S MBs synergistically enhanced the antitumor efficiency by bubble cavitation and diffusion of high-concentration H_2S intratumorally. This work provides the paradigm that the post-released gaseous MBs not only act as the contrast agents for US imaging, but also function as the therapeutic agents on combating tumor. CO_2 nanobubbles were generated from gas-generating polymeric nanoparticles by the degradation of carbonate side chain, which further infused with each other to form MBs for effective US imaging both *in vitro* and *in vivo* [81].

Typically, the enhanced ultrasonography is based on the phase-transformable nanosystems with the specific capability of post-generation of large gaseous MBs. Comparatively, the large-sized MBs could also be *in-situ* transformed into nano-sized nanobubbles for facilitating the accumulation into tumor tissues. On this ground, porphyrin MBs (designated as pMBs) were synthesized by using a porphyrin-lipid as the shell material to encapsulate a perfluorocarbon gas [69]. These pMBs acted as the desirable contrast agents for ultrasonography, and the porphyrins components provided PA and fluorescence contrast. The intriguing property of these pMBs was their response to conversion US, which converted from MBs to form nanosized bubbles for enhancing the tumor retention of these nanobubbles, keeping the same optical property of initial MBs for both PA and fluorescent imaging. After the intravenous administration of pMBs into KB xenograft-bearing mice, the US imaging clearly showed contrast enhancement by pMBs circulation into the tumor. After the direction irradiation of conversion US, the obvious decrease of US signal in tumor was observed under the contrast mode because of the conversion of large MBs into small nanobubbles. However, the direction conversion of pMBs into nanobubbles promoted the retention of nanobubbles into

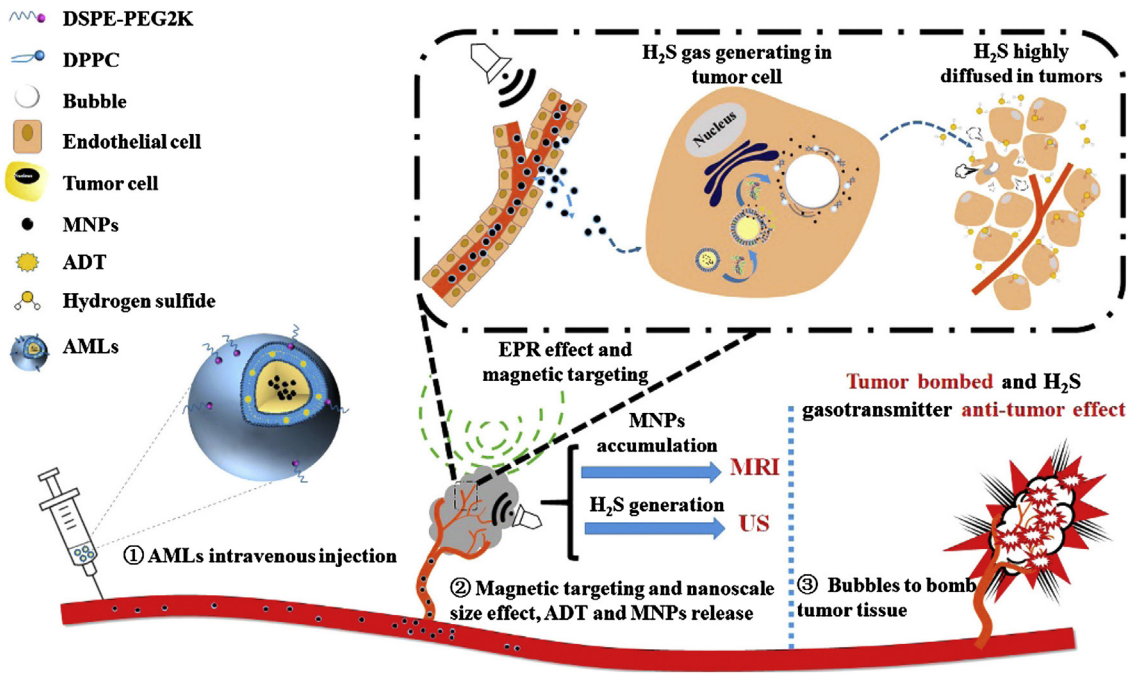

Fig. 4. Schematic illustration of the composition of AMLs, and their transformation from nanoscale particles to micrometer-sized H_2S bubbles for synergistic cancer therapy under the guidance of both MR imaging and ultrasonography.
Adapted from Ref. [80] with permission of American Chemical Society, Copyright 2017.

the tumor, inducing the continuous PA imaging of tumor [69]. In another strategy of therapeutic purpose, folate-functionalized MSNs were loaded into MBs for targeted tumor therapy [82]. Upon external US irradiation, these MSNs-loaded MBs were destructed to release the loaded nanosized MSNs, which further targeted to cancer cells by folate receptor-mediated endocytosis. Especially, such a "big-to-small" change surmounted the vascular endothelial barrier to easily enter the tumor tissue, achieving high tumor-suppressing efficiency with the assistance of US and targeted MSNs-loaded MBs [82].

Intrinsic US-responsive property of nanomedicines for US imaging

Most contrast agents for ultrasonography is based on organic MBs, nanobubbles or micro/nanoparticles. Compared to these organic micro/nano-platforms, inorganic micro/nanoparticles are featured with much higher stability, unique physiochemical property and versatile multifunctionalities. Especially, inorganic silica-based micro/nanoparticles have been extensively explored as the contrast agents for US imaging [83,84]. The rational construction of hollow nanostructure in either silica or mesoporous silica further improves the contrast-enhanced US imaging capability [85], which is also dependent on their shell stiffness [86,87], porous nanostructure [88] or multi-shell nanostructure [89].

As discussed above, MBs can significantly improve signal-to-noise ratios, but their large size and poor stability have severely hindered their applications as US contrast agents. To address this issue, superhydrophobic MSNs with large surface areas and excellent biocompatibility were designed as reliable bubble precursors and promising contrast agents by generating bubbles persistently *in situ* [90]. As illustrated in Fig. 5a, the interfacial nanobubbles on the superhydrophobic surfaces and mesopores remained stable and transformed into MBs upon exposure to US pressure above a certain mechanical index (MI). Unfortunately, this strategy provided limited contrast enhancement owing to the size and dispersity of superhydrophobic MSNs. Alternatively, an efficient nanoscale ultrasound contrast agent was fabricated using air-filling MSNs (P-hMSN) with octyl groups functionalization and amphiphilic copolymer stabilization (Fig. 5b) [91]. Upon exposure to HIFU waves, micrometer-sized bubbles were formed from air pockets inside the mesopores, which grew further outside hydrophobic MSNs (Fig. 5c). As a promising *in vivo* US contrast agents, silica nanoparticles were explored to label stem cells due to their high stability, excellent biocompatibility, and tunable morphology. Exosome-like silica (ELS) nanoparticles provided enhanced affinity to human mesenchymal stem cells (hMSCs) because of their positive charge and increased echogenicity (Fig. 5d) [92]. The ELS-labelled hMSCs were subcutaneously administrated into nude mice. In comparison with control groups (PBS and unlabelled cells), more obvious signal of echogenicity of ELS-labelled stem cells was observed from *in vivo* US images (Fig. 5**e**–h). This special nanostructure enhances the cell contrast and enables real-time cell imaging by US. Especially, the integration of silica nanoparticles with magnetic iron oxide nanoparticles achieved dual-modality nanoprobes with simultaneous US imaging and T_2-weighted MR imaging capability (contributed by iron oxide) [93]. We also demonstrated that the dispersion of ultrasmall manganese oxide nanoparticles into mesoporous of MSNs could construct multifunctional nanoprobes for both US imaging and tumor microenvironment-responsive T_1-weighted MR imaging (contributed by manganese oxide) [94].

US imaging based on genetic-coded gas nanostructures of microorganisms, including bacteria and archaea, was proposed as a non-invasive imaging protocol in biomedicine. The interaction mechanism between these nanostructures and gases is completely distinct from that of traditional MBs. The pre-loaded gas was captured by MBs and water was removed at the same time, but the 2-nm protein shell allowed the gas to spread allodially (Fig. 6a) [95]. In various optical densities (OD 0.25–2.0), compared with buffer controls, there was a striking contrast in both two kinds of gas vesicles (Fig. 6b–c). In addition, F scattering and attenuation of Ana and Halo vesicles were distinct. The echo effect of the chamber was demonstrated by the inability of contrast-enhanced US imaging to

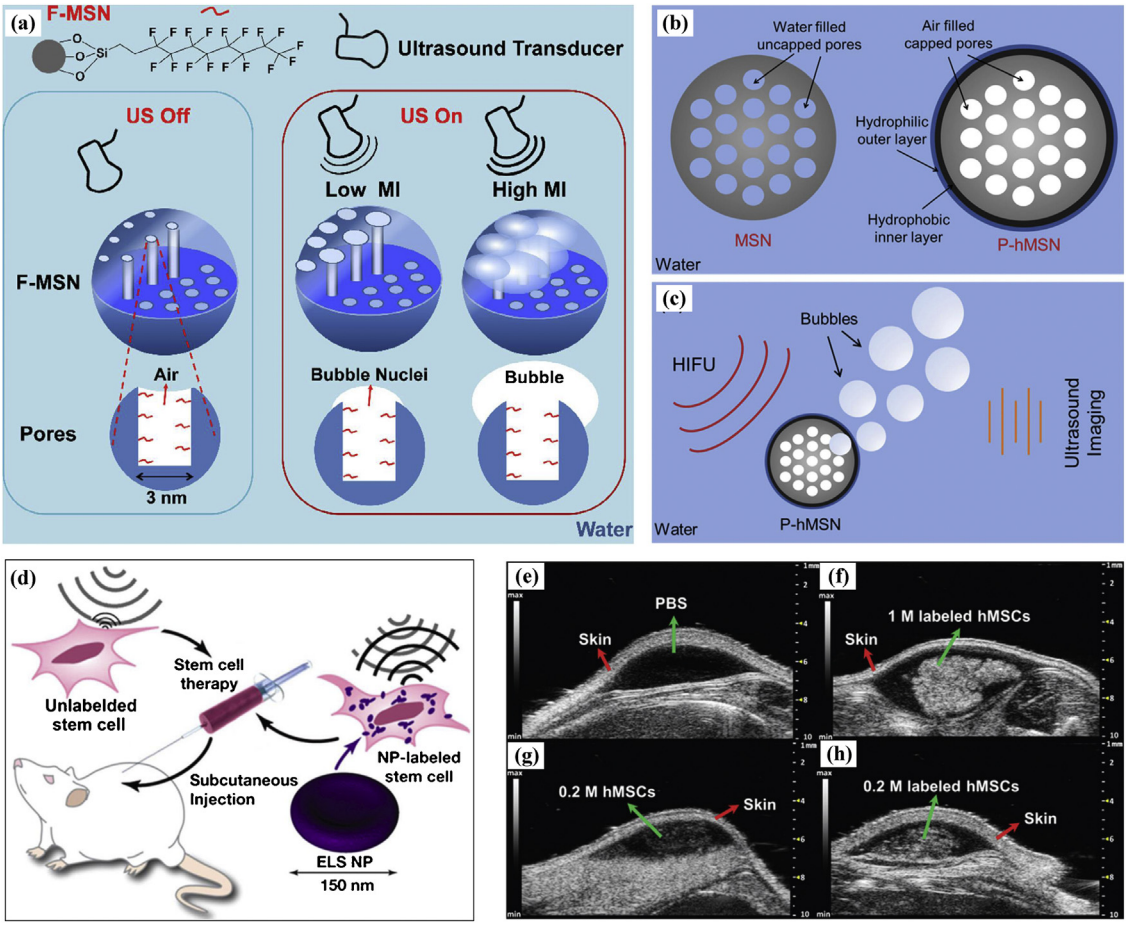

Fig. 5. (a) Schematic representation of the proposed mechanism of bubble generation from superhydrophobic MSNs. Adapted from Ref. [90] with permission of Elsevier, Copyright 2017. (b) Schematic illustration of MSNs and hydrophobic MSNs with porous structure (P-hMSN). (c) Schematic illustration of bubble formation upon exposure to HIFU sonication. Adapted from Ref. [91] with permission of WILEY-VCH Verlag GmbH & Co. KGaA, Weinheim, Copyright 2016. (d) Schematic illustration of quantification of cells echogenicity of human mesenchymal stem cells (hMSCs). *In vivo* US images of (e) PBS, (f) 1 M labeled hMSCs, (g) 0.2 M unlabled hMSCs, and (h) 0.2 M labeled hMSCs. Adapted from Ref. [92] with permission of Royal Society of Chemistry, Copyright 2017.

display the bubbles that collapsed hydrostatically (Fig. 6b–c). Then, the gas vesicles or buffer control was hypodermically injected into the lower abdomen of CD-1 mice, and the second harmonic patterns was obtained. *In vivo* US imaging showed striking enhancement on the gas vesicle side (Fig. 6d–e), but not on the control side. The contrast disappeared when US pulses were applied under overpressure (650 kPa) (Fig. 6f), confirming that vesicles were the source of contrast. Meanwhile, dynamic imaging of Halo gas vesicles (50 ml, OD 6.0) injected into caudal vein of nude mice with immune deficiency showed that in the non-linear contrast patterns (Fig. 6g), after 5 s of injection, the inferior vena cava exhibited poignant scattering. Then, as expected, the unmodified nanostructures achieved a steady condition after 50 s, and the contrast of gas vesicles was mainly intrahepatic collections (Fig. 6h). The high-power pulse of sensor absolutely eliminated the cumulative contrast (Fig. 6i). As a promising new type of US molecule reporter, the capability of gas vesicles to produce stable contrast at sub-Namo concentration might lead to more applications of US in imaging research [95]. Because of the intracellular detectability of gas vesicles, it might be developed as a reporter gene for tracing bacterial or mammalian cells, which is more suitable for long-term monitoring than traditional MBs. In addition, the physical properties of bubbles from different species, such as rapidly adjusting collapse pressure and harmonic scattering, were different, and new detection schemes could be realized. However, the biosafety of these gas vesicles for potential clinical and preclinical applications needs further study.

In addition, photosynthetic organisms, as a means of regulating buoyancy, enable this widely used non-invasive US imaging model to visualize genetically modified bacteria in living animals [96]. Non-invasive imaging of *E. coli* and *Salmonella typhimurium* was performed at a resolution of less than 100 microns when the volume density of *E. coli* and *Salmonella typhimurium* was less than 0.01%. This is due to the heterologous expression of engineered gene clusters encoding gas vesicles, which makes it possible for deep visualization of microbial cells in mammalian hosts, thus promoting the study of mammalian microflora and therapeutic cytokines. In order to compare the results of US imaging and bioluminescence imaging of ARG-expressing bacteria in gastrointestinal tract, ECN cells expressing arg1 or lux were injected into the colon of mice. To study the spatial distribution of bacteria in the colon, arg1 and lux cells were injected into the center or periphery of the colon cavity (Fig. 6j–m). US imaging patterns clearly demonstrated the localization of ECN cells (10^9 cells ml^{-1}) expressed by ARG in the proper area of colon (Fig. 6j–l), which was lower than that of ECN in gnotobiotic models. In contrast, bioluminescent patterns illustrated that bacteria existed only in the abdomen of mice (Fig. 6k–m). This suggests that genetic engineering could be used to generate ARGs with different acoustic characteristics and optimize the stability.

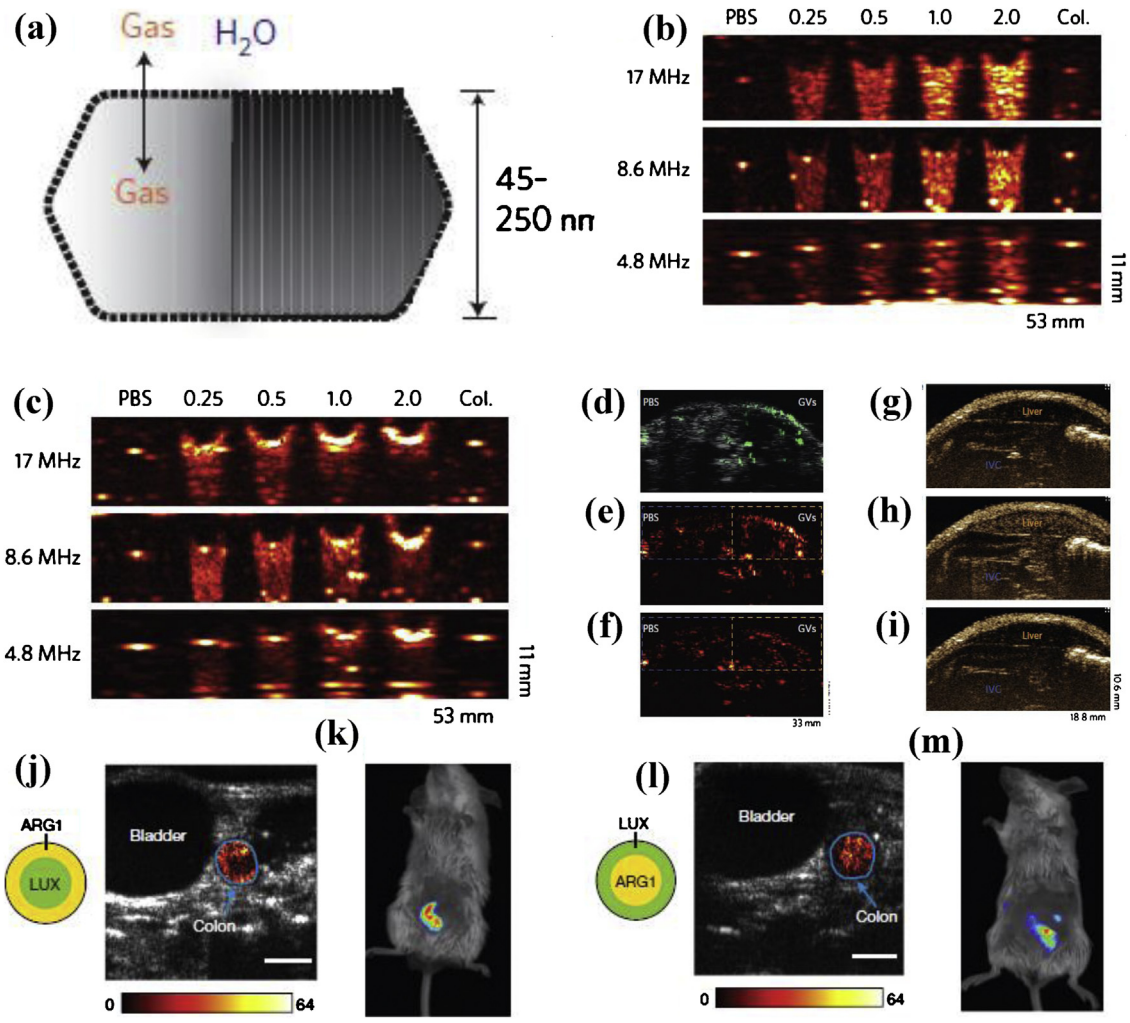

Fig. 6. (a) Schematic demonstration of a gas mediums: a gas-pervious protein shell (costate hachure) encircles a hollow gas nano-chamber (solid hachure). US imaging patterns of a gel model (including PBS buffer), Ana gas mediums (from optical densities 0.25–2) or broken down ANA gas mediums with an OD 2.0 (b) and Halo gas mediums (from OD 0.25–2) or broken down Halo gas mediums with an OD 2.0 (c). Images of different frequencies. The bottom right corner of images suggests the magnitude of each field of view. (d) Green-covered second-harmonic images with 6 MHz pulse injected hypodermically with OD 6.0 Halo balloonon (150 ml) on the right side and equivalent volume of PBS on the left side on the gray-scale broadband anatomical images of the lower abdomen of mice. (e, f) Second-harmonic US patterns with devastating insonation (650 kPa) before (e) and after (f) medium break down. Regions of interest (ROI) was used to quantify signals as dotted outlines indicated. (g, i) Non-linear contrast patterns obtained by intravenous injection of OD 6.0 Halo gas mediums (50 ml) into SCID nude mice, as obtained by using a high frequency US scanner system (manipulating at 18 MHz and 2% power). The contrasts at 4.5 s (g) and 64 s (h) were displayed by patterns after the start of injection or after the utilization of short pulse (i).

Adapted from Ref. [95] with permission of Nature Publishing Group, Copyright 2014. (j) Transverse US imaging pattern of mice, showing that the colon contained ECN expressing arg1 near the colon wall and ECN expressing lux in the lumen centrally. (k) Luminescent patterns of mice whose colonic bacterial were the same permutation. ECN expresses arg1 in the lumen centrally (1) and ECN expresses lux around (m) as shown in (j) and (k). In (j) and (1), the differential thermograms of US contrast in objective colon area before and after the acoustic break down were covered on the grayscale anatomical patterns. In (k) and (m), a threshold illuminated diagram was superimposed on the bright field image of the mouse. Imaging experiments were repeated three times *in vivo* with parallel results. Adapted from Ref. [96] with permission of Nature Publishing Group, Copyright 2018.

In addition, it could also be used to host the loading of ARGs, and express them in a wider range of microbial species. Moreover, ARG is suitable for high throughput screening based on colonies, suggesting that this new technology might have a similar trajectory [96].

Phase-changeable property of nanomedicines for US therapy

It has been well demonstrated that traditional MBs are effective not only in US imaging, but also in US-based therapeutic applications. The large particle size of MBs, however, also severely hinders their performance in US-based therapeutics. To overcome the critical issue of large particle size of MBs, various particles in the nanoscale range have been developed for US-based therapeutic applications, such as organic nanoemulsion, PLGA nanoparticles, inorganic silica nanoparticles, iron oxide nanoparticles, *etc*. However, these nanoparticles have low US responsiveness, causing limited US-theranostic efficiency. On this ground, the design of phase-changeable nanoplatforms is expected to solve this critical issue. On one hand, these nanoplatforms can easily transport within the blood vessel because of their nanoscale size. On the other hand, they can be transformed to micrometer-sized particles or bubbles based on their phase-changeable property, which is possibly realized by either intrinsic disease microenvironment or external physical triggers, leading to significantly enhanced or intelligent US-based disease therapeutics.

The gas-generating property of US-responsive nanoplatforms could be further explored for achieving US-guided therapeutic application by integration with diverse therapeutic modalities. For instance, photosensitizer chlorin e6 (Ce6)-loaded CO_2-generating

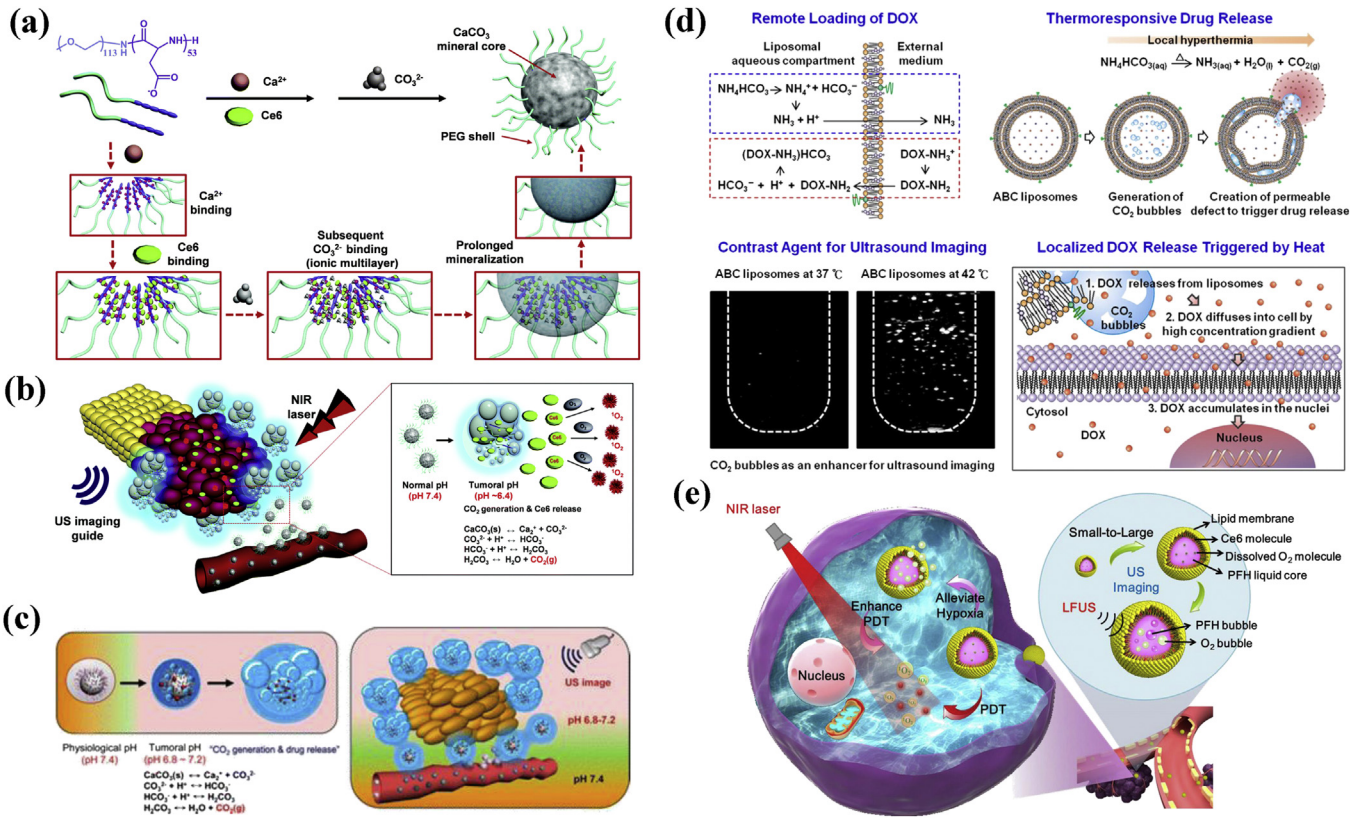

Fig. 7. (a) Schematic illustration of the fabrication of photosensitizer Ce6-loaded $CaCO_3$-mineralized nanoparticles by mineralization process, and (b) pH-responsive generation of CO_2 bubbles for US imaging and Ce6 release for PDT after potential accumulation of these nanoparticles into tumor tissue. Adapted from Ref. [97] with permission of Royal Society of Chemistry, Copyright 2016. (c) The scheme of acidity-triggered CO_2 generation from DOX-loaded $CaCO_3$ nanoparticles for US-guided chemotherapy with acidity-responsive drug-releasing performance. Adapted from Ref. [98] with permission of American Chemical Society, Copyright 2015. (d) Schematic illustration of thermo-responsive liposomes for CO_2 bubble generation, acting as the contrast agents for US imaging and heat-triggered localized extracellular DOX release. Adapted from Ref. [99] with permission of American Chemical Society, Copyright 2013. (e) The scheme of PFH@Ce6@O_2-based nanosystems for acidity-induced fusion, LFUS-triggered phase change of loaded PFH for ultrasonography and O_2 delivery for enhancing PDT efficiency on killing the cancer cells and suppressing the tumor growth. Adapted from Ref. [100] with permission of Elsevier, Copyright 2018.

calcium carbonate ($CaCO_3$)-mineralized nanoparticles were fabricated for US imaging-guided photodynamic tumor therapy (Fig. 7a–b) [97]. The $CaCO_3$ mineralization was based on anionic PEG-PAsp as the template where calcium cations (Ca^{2+}), carbonate ions (CO_3^{2-}) and Ce6 photosensitizers were involved during the synthesis (Fig. 7a). When these nanoparticles accumulated into tumor tissue, the mild acidic condition in tumor triggered the decomposition of $CaCO_3$ for CO_2 gas generation, which acted as the contrast agents for US imaging. This CO_2 gas-generating process also triggered Ce6 release for achieving enhanced efficacy of photodynamic tumor therapy. Similarly, chemotherapeutic drug doxorubicin (DOX) was concurrently loaded into $CaCO_3$ hybrid nanoparticles by the block copolymer-templated mineralization process [98]. These DOX-loaded $CaCO_3$ hybrid nanoparticles not only generated CO_2 bubbles for contrast-enhanced US imaging under the mildly acidic tumor microenvironment, but also quickly triggered the release of loaded DOX for chemotherapy by the solid-gas phase-changeable process (Fig. 7c), which achieved effective US imaging-guided antitumor efficiency both *in vitro* and *in vivo* on tumor-bearing mice.

In addition to aforementioned $CaCO_3$ nanoparticles for pH-responsive CO_2 bubble generation as the contrast agents for US imaging, ammonium bicarbonate (ABC) was capable of CO_2 generation by elevated temperature (42 °C) for triggering the decomposition of ABC [99]. ABC was encapsulated into a liposomal formulation with the co-loaded chemotherapeutic drug DOX (Fig. 7d). Upon elevating the localized temperature to 40 °C or above, the encapsulated ABC decomposed to produce CO_2 bubbles, which acted as the contrast agents for US imaging. Especially, the post-generated CO_2 bubbles created the permeable defects in the lipid bilayer for quickly triggering DOX releasing. Therefore, such a CO_2 bubble-induced contrast-enhanced US imaging provided the possibility for monitoring the thermosensitive drug release [99].

Based on the high affinity to O_2, the hydrophobic perfluorocarbon liquid has been developed as an artificial bold substitute, which was further developed as the theranostic nanoagents not only for US imaging, but also for alleviating the tumor hypoxia (Fig. 7e) [100]. PFH@Ce6@O_2-based nanosystem was fabricated by loading PFH into preformed liposomes under sonication followed by bubbling O_2 gas into as-prepared PFH@Ce6 nanoparticles. The fabricated PFH@Ce6@O_2 nanoparticles fused with each other in the form of acidity-responsive liposomal growth based on the presence of functional membrane materials, which was further triggered by low frequency US (LIFU) for activating the liquid-gas phase change of PFH and subsequently enhancing the contrast-enhanced ultrasonography. The desirable activatable US imaging was demonstrated by *in vivo* tumor ultrasonography under harmonic mode. Especially, the O_2 storage and delivery property of PFH@Ce6@O_2 significantly enhanced the Ce6-based PDT efficiency by alleviating the tumor hypoxia as demonstrated by significantly inhibited tumor growth on 4T1 tumor-bearing mice [100].

HIFU can ablate tumor tissue based on thermal and mechanical effect of US as the external physical trigger, but its therapeutic efficiency on deep-seated tumor is still low because of the US energy

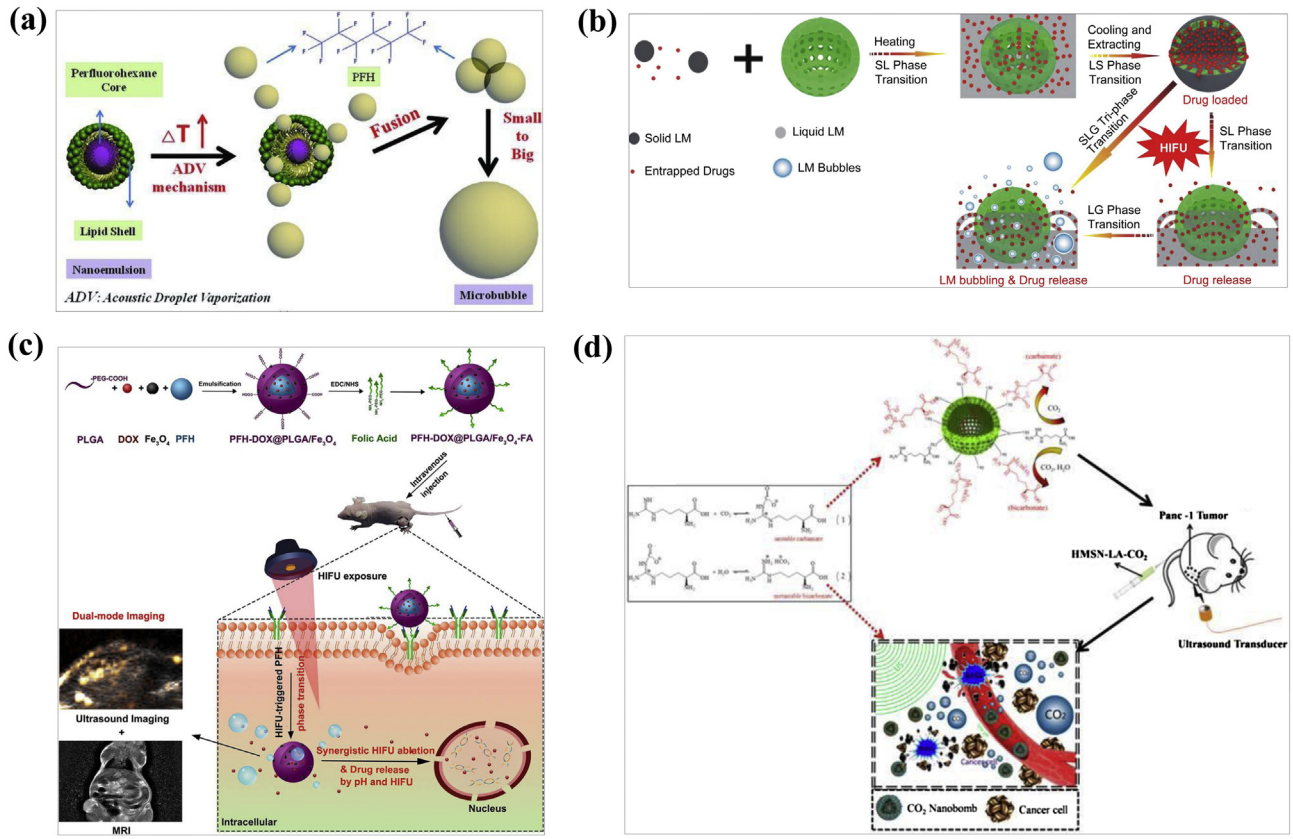

Fig. 8. (a) Schematic illustration of the phase-changeable property of PFH-loaded nanoemulsion for thermal effect-induced gaseous vaporization by HIFU irradiation based on the typical "small-to-big" strategy for US-guided synergistic HIFU ablation.

Adapted from Ref. [101] with permission of WILEY-VCH Verlag GmbH & Co. KGaA, Weinheim, Copyright 2013. (b) The scheme of chemodrug and LM co-loaded hollow MSNs for HIFU-triggered release of drugs and synergistic HIFU enhancement by mild solid-liquid-gas tri-phase transition. Adapted from Ref. [102]. with permission of Elsevier, Copyright 2014. (c) The design principle for the fabrication of PFH/DOX@PLGA/Fe_3O_4-FA composite nanoparticles for FA-targeted US/MRI dual-modality imaging and synergistic chemotherapy and HIFU against cancer. Adapted from Ref. [103] with permission of American Chemical Society, Copyright 2018. (d) Schematic illustration of the fabrication of HMSN-LA–CO_2 nanobomb with temperature and pH dual-responses for inhibiting the growth of panc-1 tumor by CO_2 bubble explosion-induced inertial cavitation. Adapted from Ref. [104] with permission of Ivyspring International Publisher, Copyright 2015.

consumption during its propagation. MBs have been demonstrated to enhance the efficacy of HIFU ablation [105,106], but they can only exert the function in the blood vasculature of tumor because of their large particle size, accompanied with the short blood-circulating time attributing to the easy capture by the reticuloendothelial systems (RES). The rational design of phase-changeable nanoplatforms was expected to synergistically enhance HIFU ablation outcome. For instance, PFH with the boiling point of 56 °C was encapsulated into organic nanoemulsion. Upon external HIFU irradiation, the thermal effect of HIFU triggered the phase change of loaded PFH from liquid to gas, which induced the PFH MBs generation and further enhanced the HIFU ablation efficacy (Fig. 8a) [101]. *In vivo* evaluation achieved nearly 6.3 times increase of the ablated tumor volume after the intravenous injection of PHF-loaded nanoemulsions based on nude mice bearing ovarian cancer, demonstrating the effectiveness of this PFH-based phase-changeable nanoemulsions as the synergistic agents for HIFU ablation. In addition to organic phase-changeable nanoemulsions, inorganic MSNs with large hollow interior were developed as the PFH-loading nanoagents for the construction of phase-changeable synergistic agents on enhancing HIFU-ablating efficacy [52]. The large hollow interiors of MSNs provided the reservoirs for hydrophobic PFH and the inorganic silica shell was featured with higher stability as compared to traditional organic nanocarriers. These PFH-loaded inorganic phase-changeable nanoagents were demonstrated to enlarge the ablation volume on VX2 liver tumor xenograft on rabbits upon HIFU irradiation. Phospholipid-stabilized hydrophobic MSNs (100 nm in size) with air-filled mesopores were efficiently internalized into cancer cells, which was also acoustically active. The low-dose HIFU insonation efficiently induced the cell death based on the acoustically produced bubbles from these hydrophobic MSNs without significant temperature elevation [43].

We also functionalized mesoporous silica-based phase-changeable nanoparticles by manganese oxide (MnO_x) components for achieving MRI-guided synergistic HIFU ablation [13]. MnO_x components acted as the contrast agents for T_1-weighted MR imaging, which assisted FUS to be precisely located onto the targeted tumor tissue. This strategy reduced the possibility of HIFU damage to the normal tissues or incomplete tumor ablation based on the fact that the boundary of tumor and normal tissue was clearly presented by the contrast-enhanced MR imaging. In addition, these PFH-loaded multifunctional inorganic phase-changeable nanoagents also enhanced the HIFU ablation outcome. To overcome the uncontrollability of explosive phase-changeable process of PFH-loaded nanoagents, a unique phase-changeable nanoplatform with mild and controllable "solid-liquid-gas" tri-phase transition behavior was elaborately designed for synergistic HIFU ablation [102]. L-menthol (LM) as the natural solid medium was loaded into the hollow interior of MSNs, which controllably and mildly transformed from solid to liquid and further to gaseous status for improving the HIFU-ablating efficacy, in accompany with the drug-loading capacity for synergistic HIFU-mediated temperature-sensitive chemotherapy and HIFU ablation (Fig. 8b).

Especially, we recently integrated several functional components into single phase-changeable nanoplatform for achieving targeted (folic acid, FA), MRI-guided and synergistic HIFU-based tumor therapy. PFH was also chosen as the "liquid-gas" phase-changeable substrate, which was loaded into PLGA nanoparticles, in accompany with the co-loaded superparamagnetic Fe_3O_4 nanoparticles for T_2-weighted MR imaging and doxorubicin (DOX) as the chemotherapeutic agents (designated as PFH/DOX@PLGA/Fe_3O_4-FA, Fig. 8c). This paradigm demonstrates the possibility of integrating multifunctional components into one US-responsive nanosystem for satisfying varied biomedical purposes [103]. Especially, the explosion of post-generated bubbles by phase-changeable process also induced cancer-cell death. Alternatively, CO_2 was initially immobilized into LA-loaded hollow MSNs (HMSNs), which was triggered by either pH change or temperature variation to desorb and release CO_2 (Fig. 8d). Low intensity US (1.0 W/cm^2) was used to induce the explosion of CO_2 bubbles based on the locally generated hyperpyrexia and shock waves. Such an explosion process induced some unique biological effects such as cavitation effect, mechanical effect and shock waves, which induced the death of panc-1 cancer cells and destruction of blood vessels in panc-1 tumor, and finally inhibited the tumor growth efficiently.

The phase-changeable micro/nanoparticles are highly promising for US-based theranostic biomedicine. They not only solve the critical issue of large particle size of traditional MBs, but also contribute more to the development of US-based therapeutic modality such as the emerging US-triggered drug release, synergistic HIFU ablation and sonodynamic tumor therapy. However, there phase-changeable micro/nanoparticles typically require exogenous or endogenous triggering to achieve phase transition and exert the functionality, which is relatively difficult to be conducted and controlled *in vivo*. Most of the aforementioned paradigms are still at the stage of conceptual demonstration. Therefore, more practical US-responsive theranostic nanomedicines with phase-changeable property should be explored in the following researches.

Intrinsic US-responsive property of nanomedicines for US therapy

In addition to the aforementioned physiochemical property of US-responsive nanomedicines for US imaging, the corresponding US-responsive property can be rationally designed for US therapy. For instance, magnetic nanoparticles with the size of 10–300 nm improved the effectiveness of US-triggered hyperthermia based on additional attenuation and scattering of US [108]. It has been well demonstrated that US can activate nanosized sonosensitizers, which produces large amounts of reactive oxygen species (ROS) for killing cancer cells. This unique US-triggered therapeutic modality is generally termed as SDT as compared to mostly explored light-triggered PDT. This SDT effect is more practical than PDT because of the high tissue-penetrating capability of US, which is induced by the cavitation effect of US to emit sonoluminescence or pyrolysis process, causing the ROS production from sonosensitizers [109–112]. Biocompatible TiO_2 nanoparticles

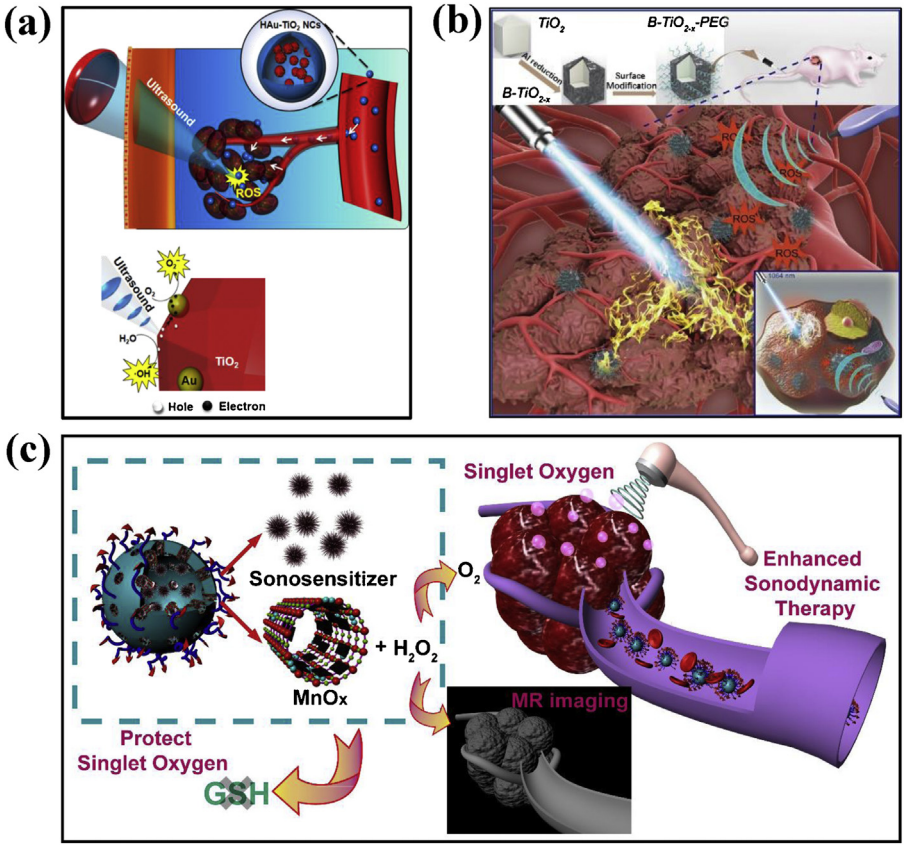

Fig. 9. Three paradigms of enhancing the SDT effect of nanosonosensitizers, including (a) Au conjugation with TiO_2 nanoparticles for improving the generation of electrons and holes upon US irradiation.

Adapted from Ref. [107] with permission of American Chemical Society, Copyright 2016. (b) Oxygen-vacancy creation of TiO_2 nanoparticles for enhancing the separation of electrons and holes upon US irradiation and synergistic therapy enabled by supplementary photothermal conversion. Adapted from Ref. [48] with permission of American Chemical Society, Copyright 2018. And (c) alleviation of tumor hypoxia by *in-situ* oxygen generation for enhanced SDT effect by multifunctional MnO_x-loaded mesoporous nanosonosensitizers. Adapted from Ref. [58] with permission of American Chemical Society, Copyright 2018.

are the mostly explored inorganic nanosonosensitizers with high response to US for generating SDT effect [113–116]. For instance, we recently fabricated biocompatible single-crystalline mesoporous titania nanoparticles (MTNs) as nanosonosensitizers for enhanced SDT [47]. The single-crystalline nature guaranteed the efficient separation of electrons (e^-) and holes (h^+) upon US irradiation, and the mesoporous structure could act as the reservoir for guest chemotherapeutic drugs. In addition, the doping of Gd component into TiO_2 nanosonosensitizers achieved T_1-weighted MR imaging-guided SDT against prostatic cancer [117].

Several strategies have been explored for enhancing the quantum yield of TiO_2-based nanosonosensitizers and subsequently improving the therapeutic efficacy of SDT. As learned from traditional photocatalysis, the surface plasmon resonance effect of Au nanoparticles prevented the electron-hole recombination of US-excited separation of electrons and holes. Therefore, the constructed hydrophilized Au-TiO_2 nanocomposites exhibited large quantity production of ROS by US irradiation, inducing the complete suppression of tumor growth (Fig. 9a) [107]. We recently demonstrated that the presence of oxygen defects in black TiO_{2-x} nanoparticles also enhanced the separation efficiency of US-excited electrons and holes, and the intriguing photothermal-conversion capability of these black TiO_{2-x} nanoparticles further synergistically enhanced the tumor SDT outcome (Fig. 9b) [48]. By construction of titania-coated Au nanoplates, these composite nanosonosensitizers realized synergistic photothermal/sonodynamic therapy of tumor, in accompany with the functionality of Au nanoplates as the electron traps to improve ROS production efficacy during SDT process [118]. For synergistic SDT, hypoxia-activated chemotherapeutic tirapazamine was loaded into hollow mesoporous TiO_2 nanoparticles with the modified S-nitrosothiol [119]. TiO_2-enabled SDT generated ROS and induced tumor hypoxia. The generated ROS sensitized S-nitrosothiol to release NO and tumor hypoxia activated tirapazamine for chemotherapy, both of which synergistically enhanced SDT efficacy.

The tumor hypoxia and corresponding reducing microenvironment significantly reduce the ROS production efficiency during SDT process. On this ground, we recently loaded MnO_x-based nanoenzyme into mesoporous nanosonosensitizers (protoporphyrin within the mesopores) for modulating the tumor hypoxia by directly transforming tumor-overexpressed hydrogen peroxide (H_2O_2) into gaseous oxygen (Fig. 9c) [58]. This strategy improved the SDT-induced ROS production and enhanced the SDT efficiency as demonstrated by the significantly suppressed growth of U87 tumor xenograft on nude mice. Liu et al. reported ultrasmall oxygen-deficient bimetallic oxide $MnWO_x$ nanoparticles for enhanced SDT against cancer by the production of singlet oxygen and hydroxyl radicals, which was based on oxygen-deficient nanostructure of $MnWO_x$ nanoparticles that acted as the electron trap site to avoid the recombination of electrons and holes [120]. Especially, the glutathione-depletion property of these nanosonosensitizers further enhanced the SDT effect on suppressing the tumor growth.

In addition to the mostly explored inorganic TiO_2 nanosonosensitizers and organic sonosensitizer-encapsulated nanosystems, other novel nanosonosensitizers have been emerging by rational design of their nanostructures, compositions and corresponding physiochemical properties. As a typical paradigm, Liu et al. demonstrated the potential of metal-organic-framework (MOF)-derived mesoporous carbon nanostructure (PMCS) in SDT augmentation (Fig. 10a and b) [121]. Such a superior sonosensitization effect of PMCS was attributed to the porphyrin-like macrocycle in MOF-derived nanostructure, which possessed large highest occupied molecular orbital (HOMO) to lowest unoccupied molecular orbital

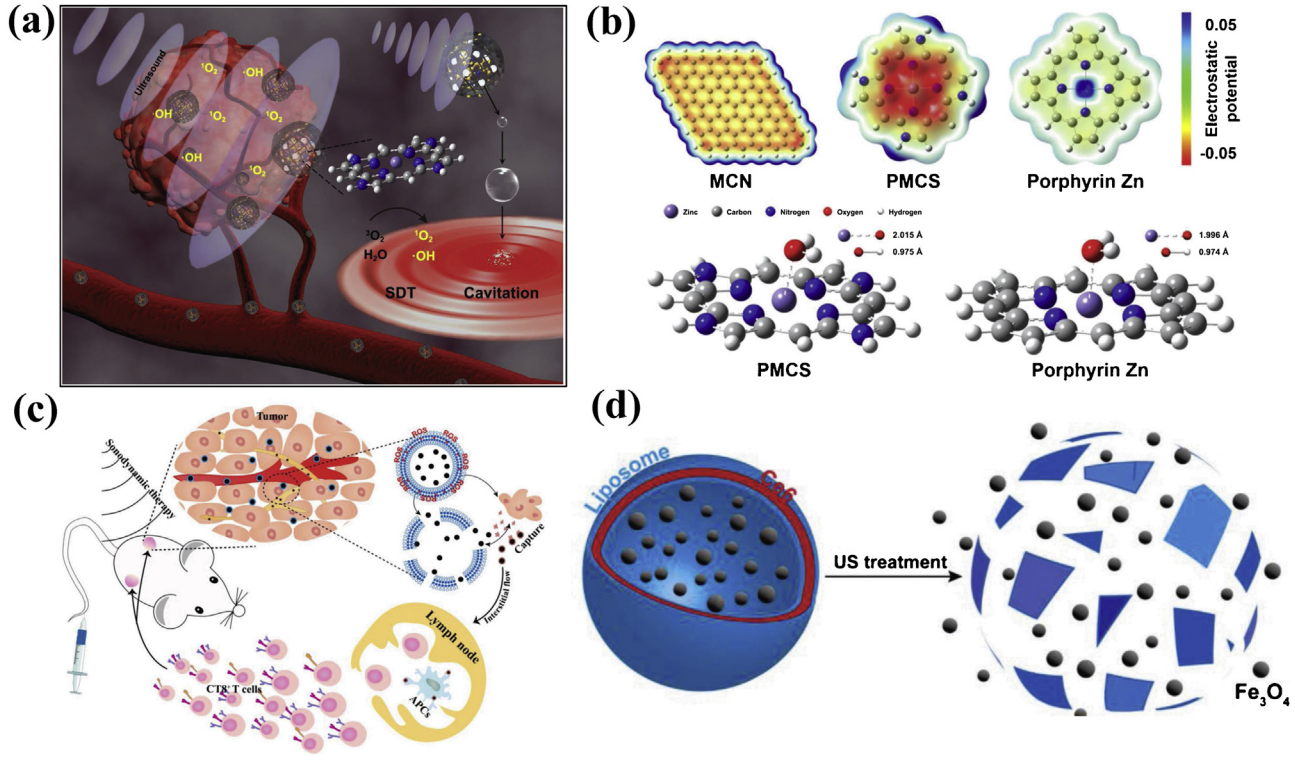

Fig. 10. (a) Schematic illustration of SDT by PMCS. (b) Density functional theory (DFT) calculations indicating mechanisms for ROS generation. Electrostatic potential profiles for MCN, PMCS, and porphyrin Zn (up), as well as the molecular models with bond length data of adsorbed H_2O on the surface of PMCS and porphyrin Zn (down). Adapted from Ref. [121] with permission of WILEY-VCH Verlag GmbH & Co. KGaA, Weinheim, Copyright 2018. (c) Schematic depiction of SDT-enhanced cancer immunotherapy. (d) Schematic illustration showing the structure evolution of Ce6/Fe_3O_4-L after US treatment. Adapted from Ref. [122] with permission of WILEY-VCH Verlag GmbH & Co. KGaA, Weinheim, Copyright 2018.

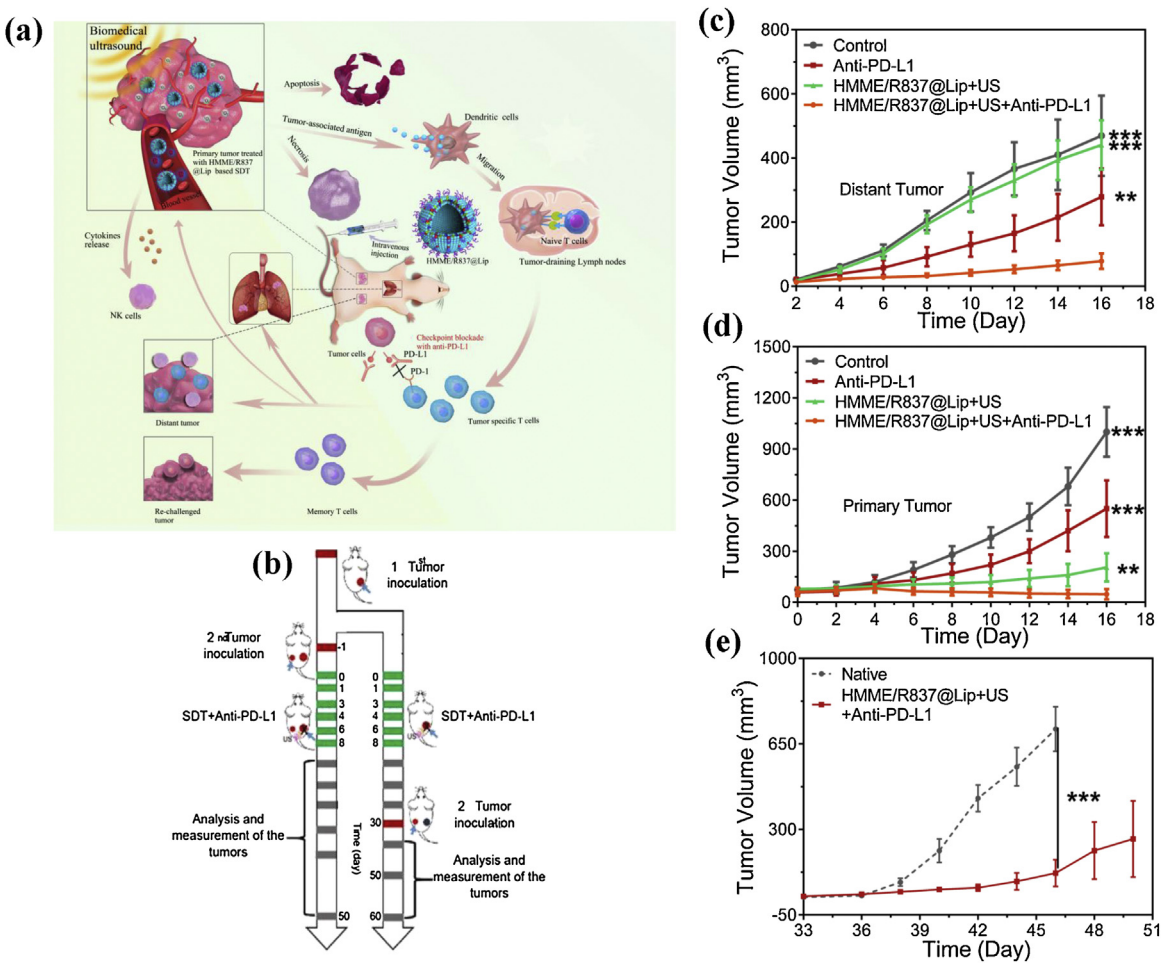

Fig. 11. (a) Schematic illustration of the combined anti-tumour immunity of checkpoint blockade and nanosonosensitizers-augmented synergistic SDT. (b) *In vivo* experiment design to assess the anti-tumour immune responses against primary/distant tumours and the immunological memory response induced by combining anti-PD-L1 and HMME/R837@Lip-augmented SDT therapy. (c) Distant and (d) primary tumour-growth curves of tumour-bearing mice after various kinds of treatments. (e) The tumour-growth curve was compared between the rechallenged tumours after the combinatorial tumour therapy and inoculated tumours of the matched native mice.
Adapted from Ref. [123] with permission of Nature Publishing Group, Copyright 2019.

(LUMO) gap that enabled highly efficient ROS generation under US treatment. Both *in vitro* and *in vivo* toxicity experiments confirmed high biocompatibility of PMCS, indicating their high application potential in cancer treatment. Recent advances in immunotherapy-based combinational therapy have inspired researchers to integrate SDT with immunotherapy for initiating remote tumor rejection by local US-treatment. Wang et al. encapsulated Ce6 and Fe_3O_4 nanoparticles (≈10 nm) into one core-shell formulation and used this nanosystem for synergistic SDT/immunotherapy (Fig. 10c and d) [122]. Especially, Fe_3O_4 nanoparticles were demonstrated with a potential for immunotherapy enhancement due to their excellent protein-capturing efficiency and lymph nodes (LNs)-targeting capability.

The encapsulation of organic sonosensitizers such as porphyrins into nanobubbles to construct US-activated therapeutic nanoagents achieved significant sonication-induced cell-ability reduction on LS 174T colorectal cancer cells because of the SDT effect [124]. In addition, rationally integrating nanosonosensitizers-augmented noninvasive SDT with checkpoint-blockade immunotherapy based construction of a multifunctional nanosonosensitizers (HMME/R837@Lip) was a highly efficient combined tumour-therapeutic modality (Fig. 11a) [123]. HMME/R837@Lip nanosonosensitizers upon implementing US irradiation killed cancer cells by inducing apoptosis and/or necrosis and further stimulated the immune system to activate the adaptive immune responses *via* HMME-augmented SDT and immune adjuvant R837-enhanced immune response. HMME/R837@Lip-augmented SDT in combination with anti-PD-L1 (Fig. 11b) was successfully demonstrated to have vigorous anti-tumour immunity, which not only efficiently arrested primary tumour progression, but also substantially prevented the mimic distant metastasis (Fig. 11c–d). Furthermore, such combined treatment strategy offered a long-term immunological memory function, which could protect against tumour rechallenge after elimination of the initial tumours (Fig. 11e), representing the proof-of-concept combinatorial tumour therapeutics based on noninvasive tumours-therapeutic modality with immunotherapy.

In addition to the mostly explored SDT for cancer therapy, SDT has also been demonstrated to be effective in the treatment of Alzheimer's disease (AD). The typical organic sonosensitizer protoporphyrin IX (PX) was loaded into oxidized mesoporous carbon nanospheres with brain-targeting peptide RVG conjugation (designated as PX@OMCN@PEG@RVGs, Fig. 12a) as the targeted nanosonosensitizer for US-activated inhibition of tau phosphorylation and Aβ aggregation [55]. The surface RVG peptide assisted the delivery of nanosonosensitizers across BBB, and the produced ROS by SDT improved the cognitive function of APP/PS1 Tg mice by introduced FUS (Fig. 12b), together with the high brain biocompatibility, initiating a new therapeutic strategy for AD treatment based on US-based nanomedicine.

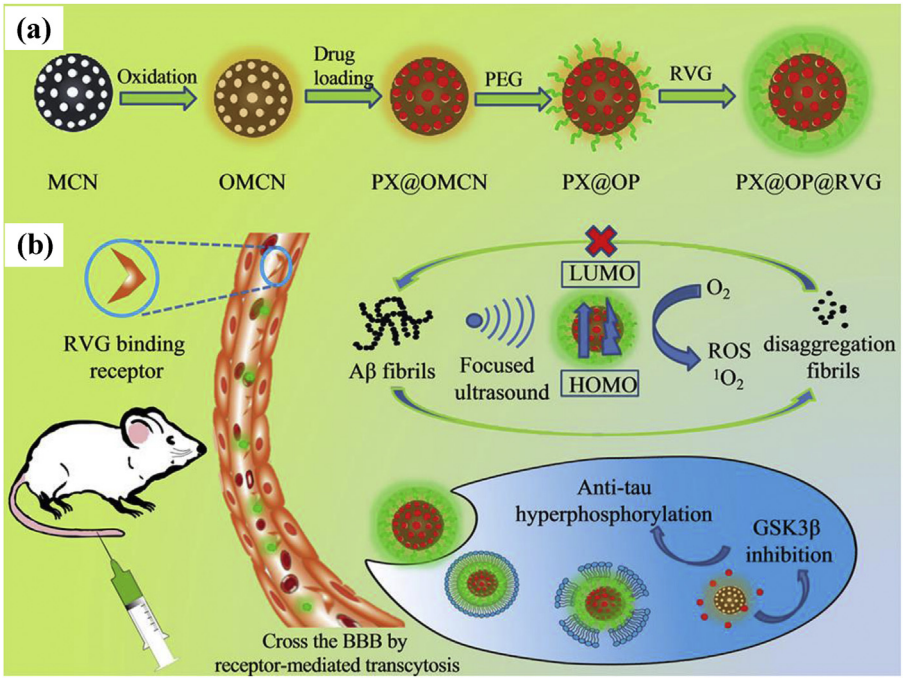

Fig. 12. Schematic illustration of (c) the synthesis of PX@OP@RVG nanoplatforms, and (d) their therapeutic functionality by receptor-mediated BBB crossing for US-triggered and SDT-induced ROS production and Aβ aggregation inhibition and Alzheimer's disease (AD) inhibition.
Adapted from Ref. [55] with permission of American Chemical Society, Copyright 2018.

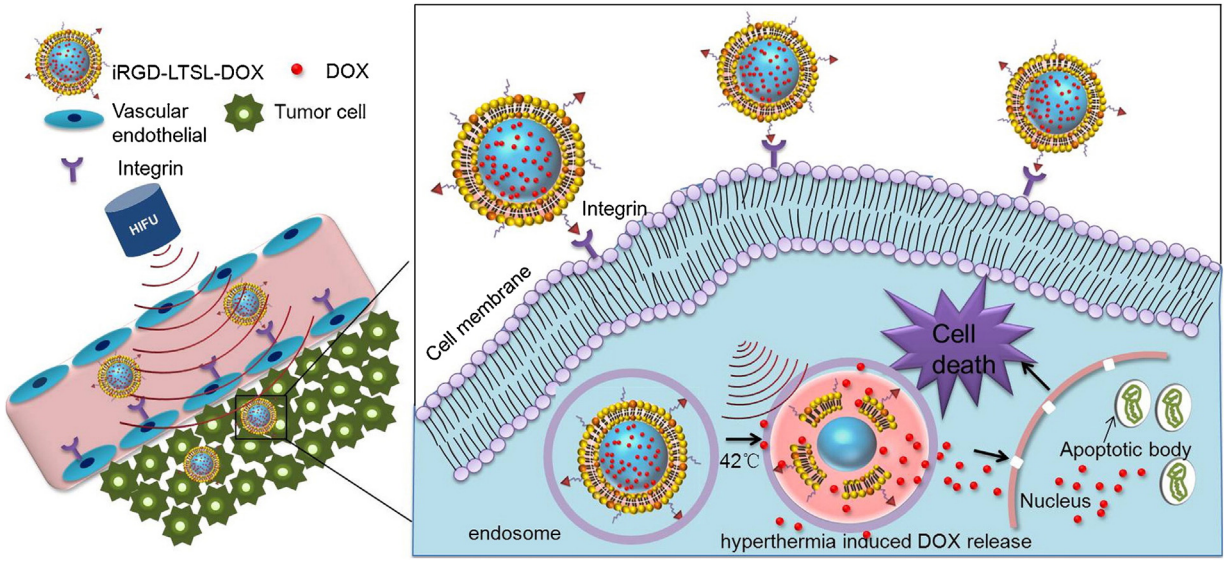

Fig. 13. Schematic illustration of the composition of iRGD-LTSL-DOX for exerting its specific functionality on targeted and HIFU-based hyperthermia-triggered drug release and chemotherapy.
Adapted from Ref. [125] with permission of Elsevier, Copyright 2016.

Compared to other external triggers (*e.g.*, light, magnetic field, electric field) for stimuli-responsive drug release from versatile nanomedicine, US is more practical because of its high tissue-penetrating depth and non-invasiveness [126–128]. By rational design of US-sensitive gatekeepers on the surface of MSNs such as the inclusion of mechanophores (tetrahydropyran) with US-cleavable bonds, the controlled release of chemotherapeutic drugs was realized on transdermal drug-delivery nanosystems [129]. Especially, the hyperthermia effect of HIFU can be exploited to stimulate the temperature-responsive drug release, featuring the synergetic therapeutic paradigm. As a paradigm, Deng et al. have constructed tumor homing peptide (iRGD) conjugated, chemodrug doxorubicin (DOX) encapsulated low temperature-sensitive liposomes (LTSL) for tumor targeted HIFU/chemotherapy combination suppression (Fig. 13) [125]. These LTSL effectively disintegrated under a mild temperature increase from 37 °C to 42 °C, promoting approximately 90% of DOX release. Such heating process was readily realized by HIFU both *in vitro* and *in vivo*. It is noted that iRGD peptide conjugated onto LTSL displayed satisfied tumor-targeting efficiency when the nanomedicine was administrated into 4T1 tumor-bearing mice intravenously. Upon localized HIFU irradiation, iRGD-LTSL-DOX treatment group received impres-

sive tumor-suppression consequences (65.2%), featuring effective therapeutics with high biocompatibility [125]. The low intensity focused US (LIFU) could activate porphyrin-phospholipid-liposome for sonosensitization-induced lipid oxidation, which further disrupted the liposome to trigger the release of loaded doxorubicin for improved drug deposition in tumor and significantly suppressed tumor growth [130]. In addition, the US-controlled pulsatile insulin release from PLGA nanocapsules regulated the blood glucose level and achieved glycemic control for long period of one week [131]. The release of nitric oxide (NO) was also be triggered from porous nanocarriers for tumor-specific and precise gas therapy [132]. In addition, US was used to trigger oxygen release from oxygen-carrying PFC nanodroplets where oxygen was absorbed in the lung during circulation, which was employed for tumor oxygenation to enhance the therapeutic efficacy of PDT and radiotherapy [133].

Biological effect of US-responsive nanomedicine

US is featured with high tissue-penetrating capability, which can also generate some unique biological effects such as thermal and mechanical effects, cavitation, pressure change and acoustic fluid streaming [134,135]. These US-specific biological effects have been extensively explored for satisfying diverse biomedical purposes, where nanomedicine has supplemented broader possibilities in disease theranostics. In addition, the intrinsic biological effect of US-responsive nanoparticles plays the determining role for guaranteeing their further clinical translation, especially for the biological toxicity issue.

Biological chemistry of US-responsive nanomedicines

The biological effects of US-responsive nanoparticles include their biodegradation behavior, possible excretion pathways, histocompatibility, and some unique effects to the specific organs or tissues [136,137]. The high biocompatibility and biosafety are the priority of designing these nanosystems [138], where the organic nanosystems currently show more promising application potential as compared to some inorganic nanoparticles. The components of some representative organic nanosystems (*e.g.*, liposomes, micelles, PLGA) have been broadly demonstrated to be biocompatible at current stage, but the inorganic nanoparticles still suffer from the unclear biological effects such as the difficulty in biodegradation [139–142]. It should be noted that some functional components should be integrated into these organic or inorganic nanosystems for achieving US response, which complicates the nanosystems and consequently makes the evaluation of the corresponding biological effects more difficult. The unclear biological effects and underlying biological chemistry of nanoparticles are one of the most hurdles for hindering their further clinical translation, which is not only in this specific US-responsive nanomedicine, but also in the whole nanomedicine-involved research field.

The underlying synthetic chemistry and surface chemistry could be potentially used to improve the biocompatibility of US-responsive nanoparticles. For instance, the adequate use of synthetic chemistry could control the dispersity, particle size and composition of these nanoparticles. The dispersity control reduces the aggregation of these nanoparticles to avoid the potential blocking of blood vessels. The composition control can control the biodegradability of nanoparticles for potentially guaranteeing the long-term biosafety. The adequate surface engineering based on surface chemistry is of high significance for determining their *in vivo* behaviors. For example, surface PEGylation can improve the stability in physiological condition and prolong the blood-circulation duration, and surface-targeting engineering can enhance the accumulation of these nanoparticles into lesion sites, both of which reduce the nonspecific distribution of these nanoparticles into normal cells/tissues, mitigating their potential side effects.

Biological effect of US for nanotheranostics

US can bring with some unique biological effects for achieving the desirable US-responsive theranostic nanomedicine. For instance, MBs-assisted focused US (FUS) can induce transient disruption of BBB reversibly [143], which has been used to enhance the delivery of therapeutic agents into brain for the treatment of brain-related diseases [144,145]. In addition, the US-induced inertial cavitation has been demonstrated to promote the extravasation of MSNs in a flow-through tissue-mimicking agarose phantom [146], which is promising to enhance the extravasation of nanoparticles out of the blood vessel to enter the tumor tissue, solving the critical issue of the difficulty in targeting tumor tissue of nanoparticles [147]. The same phenomenon was demonstrated by curcumin-loaded pluronic P123/F127 polymeric micelles where the FUS treatment enhanced the tumor permeabilization and improved the penetration of drug-loaded micelles into tumor tissues [148]. Therefore, the mechanical effect and cavitation effect of US not only enhance the penetration of extravasated nanoparticles, but also control the local drug release by pre-determined US irradiation model [149]. Especially, the well-demonstrated US-targeted MBs destruction (UTMD) technology could improve the gene-transfection efficiency and therefore enhance the gene-therapeutic outcome [150–153].

Superparamagnetic iron oxide nanoparticles exhibit high potential in MR imaging for various disease monitoring, such as tumor imaging, but rarely developed in brain disease imaging mainly due to restriction of BBB. BBB consists of closely packed endothelial cells, astrocytes, pericytes, tight junctions, and extracellular matrix components, preventing the therapeutic and toxic compounds from entering the central nervous system [156,157]. Fortunately, US-based techniques have been applied for opening BBB and permeability enhancement as assisted by MBs. For instance, ultrasmall superparamagnetic iron oxide (USPIO)-loaded MBs was used to mediate and monitor BBB permeation in association with transcranial US pulses [154]. USPIO-containing MBs were initially infused into healthy mice, followed by exposure to high MI US pulses. USPIO was released from destructed MBs, extravasated across the permeabilized BBB and accumulated into brain tissue, further providing R_2-based MR imaging of brain tissue (Fig. 14a). The R_2 values increased by 5.5% after one-minute treatment of USPIO-MB administrated group, and further increased by 14.4% and 21% after prolonged 5 min and 30 min (Fig. 14b). Therefore, USPIO-MBs compound could be employed to mediate and monitor BBB permeation in brain tissues, providing powerful support for the treatment of major brain diseases.

In addition, FUS is also capable of opening BBB for enhancing the accumulation of delivered nanoparticles into brain tumor. For instance, molecularly organic-inorganic hybrid mesoporous organosilica nanoparticles (HMONs) were decorated with ultrasmall $Cu_{2-x}Se$ nanoparticles by disulfide linker (abbreviated as HMONs-ss-$Cu_{2-x}Se$ and designated as HCu, Fig. 14c) for achieving FUS-enhanced BBB opening and synergistic therapy (Fig. 14d) of glioblastoma multiforme (GBM) [155]. By exposure to FUS irradiation, DOX-loaded HCu was accurately transported into the brain tumor as demonstrated by the obviously enhanced *in vivo* fluorescence imaging of tumor on U87 glioma-bearing mice after receiving ICG-loaded HCu (Fig. 14e and f). This work provides the paradigm that FUS not only assists the accumulation of free therapeutic drug molecules into brain, but also is effective in enhancing the nanoparticle accumulation and delivery into brain [155].

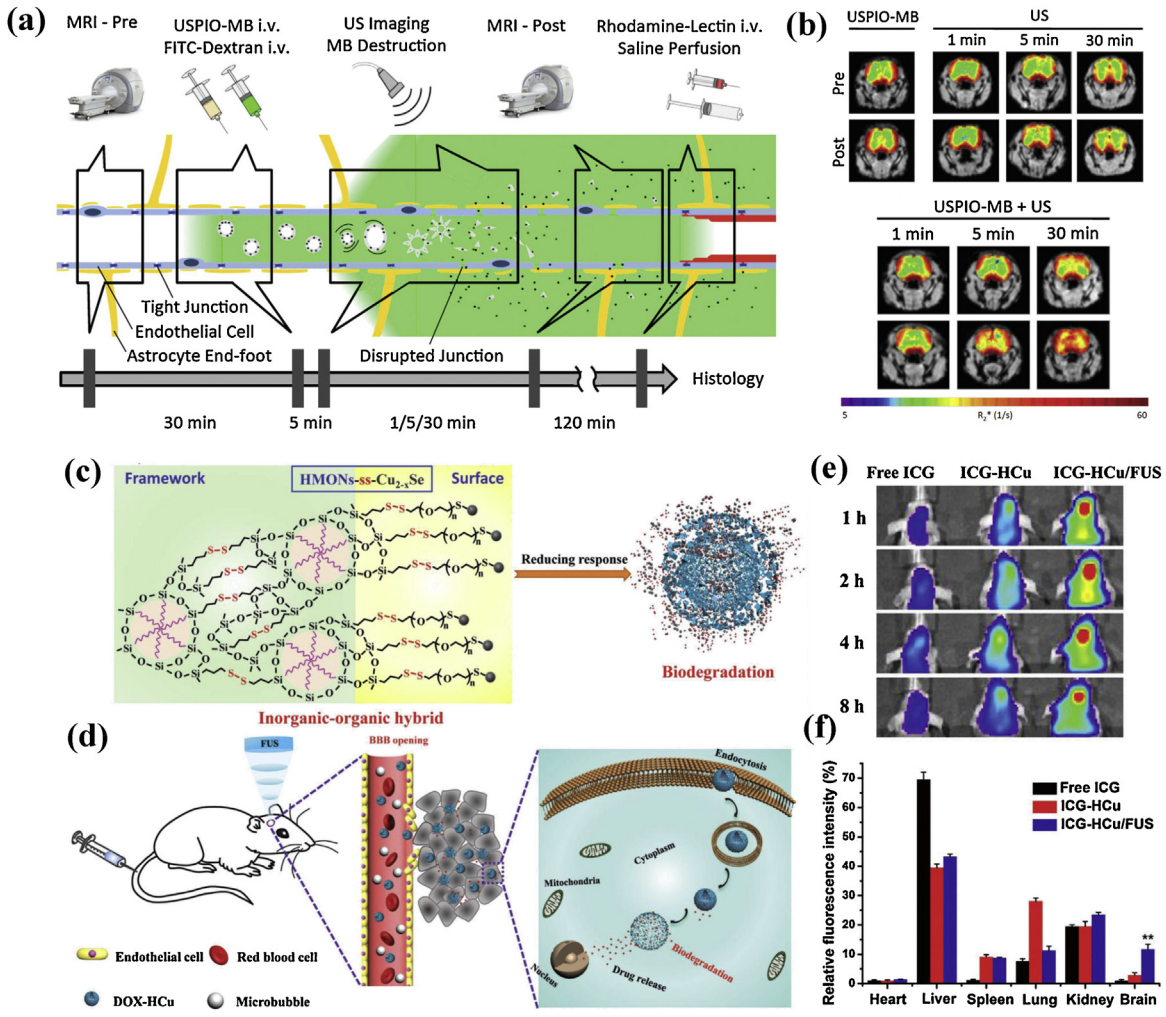

Fig. 14. (a) Schematic illustration of ultrasmall superparamagnetic iron oxide (USPIO)-loaded poly(butyl cyanoacrylate)-based MBs for mediating and monitoring drug delivery across BBB. In brief, USPIO-MB and FITC-Dextran were intravenously injected, followed by high MI US pulse, causing USPIO release and penetration across BBB. MRI was applied for visualizing USPIO deposition in the brain. (b) MR imaging and color-coded R_2-maps of brain tissue after USPIO-MB administration and US treatments. Adapted from Ref. [154] with permission of WILEY-VCH Verlag GmbH & Co. KGaA, Weinheim, Copyright 2015. (c) The scheme of the detailed composition of HMONs-ss-$Cu_{2-x}Se$ (HCu) nanoparticles and reducing-responsive biodegradation. (d) Schematic illustration of FUS-induced opening of BBB, enhanced delivery of DOX—HCu into brain tumor and TME-responsive release of therapeutic agents for PA-guided synergistic treatment of brain tumor (glioblastoma multiforme). (e) Fluorescent imaging of U87 glioma-bearing mice after receiving different agents, including free ICG, ICG—HCu and ICG—HCu combined with FUS treatment, and (f) the corresponding quantified fluorescence intensity of different organs. Adapted from Ref. [155] with permission of WILEY-VCH Verlag GmbH & Co. KGaA, Weinheim, Copyright 2018.

Based on the unique biological effect of FUS, it has been explored for the treatment of diseases in central nervous system (CNS) such as glioma therapy, neuroregeneration and neuromodulation. On this ground, US-gated nanoparticle carriers were designed for the delivery of small molecule anesthetic propofol on US-triggered neuromodulation [158]. This US-responsive nanosystem was based on the fabrication of a nanoemulsion, which was composed of polyethylene glycol-*b*-polycaprolactone block copolymer with a liquid PFC core (perfluoropentane) and the loaded drug molecules. Upon FUS irradiation, the perfluoropentane core changed from liquid to gas, causing the release of loaded therapeutic drug, which further enabled a potent neuromodulatory effect and silenced seizures in an acute rat seizure model [158]. Based on the thermal effect of high-frequency US, the surface of amine-functionalized MSNs was engineered with PEG chains by a thermo-sensitive linker [159]. The high frequency US-induced thermal effect caused the breakage of the thermo-sensitive linker and detached the surface PEG shell, which induced the exposure of surface positive charge for enhancing the cellular uptake of MSNs. The enhanced internalization of drug-loaded MSNs in human osteosarcoma cells significantly improved the cytotoxic effect of nanomedicine. Therefore, the thermal effect of US indirectly induced the biological effect of enhanced cellular uptake of internalization, potentially achieving high therapeutic efficiency.

Design principle, facing challenge and future development of US-responsive nanomedicine

US-based theranostic nanomedicine develops relatively slow as compared to other external-triggered modalities such as light activation, which is mainly attributed to the difficulty in the fabrication of nanomedicines with unique response to US exposure. Fortunately, chemistry provides the foundation of elaborately designing versatile US-responsive nanosystems or nanoplatforms for satisfying US-based biomedical applications (Table 2). First, the synthetic chemistry makes the fabrication and structure/composition optimization of these US-responsive nanoparticles possible. Second, the surface chemistry enables the surface engineering to meet

Table 2
Summative paradigms of US-responsive nanomedicine for US imaging and US therapy.

US-responsive nanosystems	US-responsive property	US-responsive theranostic modality	US-responsive theranostic outcome	Refs.
Au-PFC nanodroplets	Liquid-gas phase transition	Both PA imaging and US imaging	Dual PA and US for imaging highly optically scattering and absorbing tissues	[77]
Dye-PFH nanodroplets	Liquid-gas phase transition	US imaging	High-resolution *in vivo* ultrasonography	[78]
Pillar [6]arene-GO	CO_2 releasing	PA and US imaging	Photothermal-enhanced PA and US imaging capability	[79]
ADT-loaded nanoliposome	H_2S releasing	US imaging	Contrast-enhanced US imaging and tumor therapeutics	[80]
Porphyrin MBs	Big-to-small transition	PA and US imaging	Enhanced tumor accumulation for US and PA imaging	[69]
Superhydrophobic MSNs	Bubble generation	US imaging	Contrast-enhanced US imaging upon exposure to US pressure above a certain MI	[90]
Air-filling MSNs	Bubble generation	US imaging	HIFU-triggered contrast-enhanced US imaging	[91]
Microorganism	Gas nanostructure	US imaging	Contrast-enhanced US imaging as ultrasonic molecular reporters for long-term monitoring	[95]
$CaCO_3$-mineralized nanoparticles	CO_2 releasing	US-triggered therapy	CO_2 gas-generating process for triggering Ce6 release for achieving enhanced efficacy of photodynamic tumor therapy	[97]
PFH@Ce6@O_2	O_2 delivery and releasing	US-triggered therapy	Liquid-gas phase change of PFH for US imaging and O_2 delivery for mitigating tumor hypoxia	[100]
PFH-nanoemulsion	Liquid-gas phase transition	HIFU ablation	Synergistically enhancing the HIFU ablation efficacy of tumor	[101]
MnO_x-PFH-HMSNs	Liquid-gas phase transition	HIFU ablation	Synergistically enhancing the HIFU ablation efficacy of tumor with MRI guidance	[13]
Mesoporous titania	ROS generation	Sonodynamic therapy	Efficient ROS generation and SDT against tumor	[47]
Black TiO_{2-x}	ROS generation	Sonodynamic therapy	The presence of oxygen defects for enhancing SDT effect on tumor suppression	[48]
Mesoporous sonosensitizers	ROS generation	Sonodynamic therapy	Tumor hypoxia relief to enhance the SDT effect against tumor growth	[58]
MOF-derived carbon particle	ROS generation	Sonodynamic therapy	Highly efficient ROS generation under US treatment for tumor therapy	[121]
MSNs with surface gatekeeper	Controlled gatekeeper opening	Drug delivery	US-responsive drug release for enhanced chemotherapy	[129]
Temperature-sensitive liposomes	Controlled expansion	Drug delivery	HIFU-sensitive drug release by temperature elevation for enhanced chemotherapy	[125]

the strict requirements of biomedicine, such as guaranteeing the long-term blood circulation and positively targeted accumulation into lesion tissues. Third, the intrinsic physiochemistry of these US-responsive nanosystems is employed for US-based theranostic applications such as ultrasonography and US-based therapy. Finally, the biochemistry of US-responsive theranostic nanoplatforms induces some intrinsic biological effects, determines their biosafety/biocompatibility and guarantees their further clinical translation. Overall the rational design of these US-responsive nanoparticles should be strictly based on their aforementioned chemical principles, which has been discussed in detail on numerous representative paradigms in this review. The destination of these researches on US-responsive nanomedicine is the final clinical translation and application to benefit the patients. Although the demonstrated performances of these nanoparticles in US biomedicine is outstanding and promising, their further clinical translation still suffers from several unresolved challenges and critical issues, which is discussed below from the specific viewpoints of chemistry.

(1) From the viewpoint of material-synthetic chemistry, the large-scale, reproducible and high-quality production of US-responsive nanoparticles hasn't been achieved. Almost all these nanoparticles were fabricated in laboratory with small amount production. In addition, the precise control of the nanostructure and composition is still highly challenging and their reproducible production is a big facing problem, especially at the large-production stage. However, these nanoparticles will finally enter the clinical translation stage. Therefore, the current design principle should take some key points of design, synthesis and optimization into consideration, including the cost, synthetic difficulty, quality control, possibility for large-scale production, *etc*.. It is noted that the rapid progress of nanomedicine in the past decade has significantly promoted the exploring of new synthetic methodologies, principles and apparatus for nano-fabrications. The related techniques and lessens should be extended to the synthesis of these US-responsive nanoparticles.

(2) From the viewpoint of surface chemistry, the precise control of surface-chemical status is still highly challenging, which however is important for determining the *in vivo* behaviours of these US-responsive nanoparticles. The complex *in vivo* environment typically requires the minimal interaction of nanoparticles with substances within the blood vessel, and the specific tumor microenvironment needs the large accumulation of nanoparticles into tumor tissue. Different nanoparticles have their intrinsic surface chemistry, therefore no standard surface-engineering strategy is currently available, making it difficult for pre-determination of nanoparticles' surface status and the subsequent *in vivo* biological behaviours. In addition, the surface-targeting engineering seems promising, but the actual targeting efficiency is still rather low because of the presence of versatile proteins within the blood vessel that would be absorbed onto the surface of nanoparticles to form protein corona, lowering the targeting capability of these US-responsive nanoparticles. Therefore, the adequate surface-engineering strategies are highly urgent to be developed at current stage for delivering the nanoparticles into lesion tissues with high amount.

(3) For the viewpoint of physiochemistry, the development of US-responsive nanomedicine is far less than traditional light-responsive nanomedicine because the rational design of

nanosystems with US-responsive physiochemistry is relatively difficult. Although the phase-changeable property is effective, the quantitative evaluation and precise control of such a phase-transforming procedure have not been achieved, making it still at the research stage and difficult for further clinical translation. Some nanosystems have been demonstrated to be featured with intrinsic US-responsive property such as sonodynamic effect, but the intrinsic mechanism has not been fully revealed. Therefore, the precise modulation of US-responsive performance is challenging because of the unclear mechanism. In addition, the detailed influence of US irradiation parameters on the US-responsive performance of nanoparticles originating from their intrinsic physiochemistry has not been studied. In addition to the mostly reported tumor therapy, the exploring of these US-responsive nanomedicines for the treatment of other diseases should be further considered.

(4) From the viewpoint of biological chemistry, the biological behaviours and intrinsic biotoxicity of US-responsive nanoparticles have not been fully evaluated and revealed, especially for their influence on the normal cells or tissues. In addition, the biological effect of US on the *in vivo* behaviours of nanoparticles has not also been fully explored. It should be noted that most researches provide the preliminary data on the acute or short-term toxicity of nanoparticles, but their long-term biological effects are still unknown. Especially, the data on the excretion pathways and biodegradation behaviours of most US-responsive nanoparticles are still lacking. It is highly expected that the following researches on the biological-effect and biotoxicity evaluation should follow the rule of standard toxicity evaluation, rather than the different protocols as reported in various labs and research groups.

(5) From the viewpoint of biomedical applications, US-responsive nanomedicine mainly focused on tumor treatments. Based on the unique feature of US as the triggering source and the promising theranostic performance, it is highly expected that US-based therapeutic nanomedicine can find more biomedical applications, such as antibacterial, anti-infection, BBB opening for neuromodulation, heat-disease therapy, and even tissue engineering.

Compared to traditional photonic biomedicine, US biomedicine has found their broad applications in clinic for either disease diagnosis or therapy. Diverse US-based instruments or apparatus have been clinically used. Therefore, the development of the corresponding US-responsive nanomedicine has its clinical application base. MBs, as the unique paradigm extensively used in contrast-enhanced US imaging, establish the confidence of researchers for promoting the clinical translation of diverse US-responsive nanomedicines, if the aforementioned critical issues would be fully addressed in the near future.

Acknowledgements

We greatly acknowledge the financial support from the National Key R&D Program of China (Grant No. 2016YFA0203700), National Natural Science Foundation of China (Grant No. 81771848, 81571693, 81871361, 81901752 and 51672303), Excellent Young Scientist Foundation of NSFC (Grant No. 51722211), Shanghai Sailing Program (Grant No. 19YF1440500), Program of Shanghai Subject Chief Scientist (Grant No. 18XD1404300), Young and Middle-aged Medical Talents Project of Wuhan (Grant No. 2018-116), Wuhan Science and Technology Project (Grant No. 2017060201010181), Shanghai East Hospital "leading talent project" (Grant No. DFRC2018024) and Pudong Health Bureau of Shanghai (Grant No. PWRI2018-06).

References

[1] P.L. Rodriguez, T. Harada, D.A. Christian, D.A. Pantano, R.K. Tsai, D.E. Discher, Science 339 (2013) 971–975.
[2] H. Wang, D.J. Mooney, Nat. Mater. 17 (2018) 761–772.
[3] D. Kim, J.M. Yoo, H. Hwang, J. Lee, S.H. Lee, S.P. Yun, M.J. Park, M. Lee, S. Choi, S.H. Kwon, S. Lee, S.H. Kwon, S. Kim, Y.J. Park, M. Kinoshita, Y.H. Lee, S. Shin, S.R. Paik, S.J. Lee, S. Lee, B.H. Hong, H.S. Ko, Nat. Nanotechnol. 13 (2018) 812–818.
[4] F. Peng, M.I. Setyawati, J.K. Tee, X.G. Ding, J.P. Wang, M.E. Nga, H.K. Ho, D.T. Leong, Nat. Nanotechnol. 14 (2019) 279–286.
[5] V.P. Chauhan, R.K. Jain, Nat. Mater. 12 (2013) 958–962.
[6] M.E. Lobatto, V. Fuster, Z.A. Fayad, W.J.M. Mulder, Nat. Rev. Drug Discov. 10 (2011) 835–852.
[7] Y.L. Wang, S.Y. Sun, Z.Y. Zhang, D.L. Shi,Adv. Mater. 30 (2018), 1705660.
[8] G.S. Song, L. Cheng, Y. Chao, K. Yang, Z. Liu,Adv. Mater. 29 (2017), 1700996.
[9] S. Wang, P. Huang, X.Y. Chen, Adv. Mater. 28 (2016) 7340–7364.
[10] P.Y. Chen, Y.C. Ma, Z. Zheng, C.F. Wu, Y.C. Wang, G.L. Liang, Nat. Commun. 10 (2019) 1192.
[11] X.D. Xue, Y. Huang, R.N. Bo, B. Jia, H. Wu, Y. Yuan, Z.L. Wang, Z. Ma, D. Jing, X.B. Xu, W.M. Yu, T.Y. Lin, Y.P. Li, Nat. Commun. 9 (2018) 3653.
[12] H. Ke, J. Wang, Z. Dai, Y. Jin, E. Qu, Z. Xing, C. Guo, X. Yue, J. Liu, Angew. Chem. Int. Ed. 123 (2011) 3017–3021.
[13] Y. Chen, H.R. Chen, Y. Sun, Y.Y. Zheng, D.P. Zeng, F.Q. Li, S.J. Zhang, X. Wang, K. Zhang, M. Ma, Q.J. He, L.L. Zhang, J.L. Shi, Angew. Chem. Int. Ed. 50 (2011) 12505–12509.
[14] S.H. Noh, S.H. Moon, T.H. Shin, Y. Lim, J. Cheon, Nano Today 13 (2017) 61–76.
[15] J. Lim, S.A. Majetich, Nano Today 8 (2013) 98–113.
[16] T. Gu, Y. Wang, Y. Lu, L. Cheng, L. Feng, H. Zhang, X. Li, G. Han, Z. Liu,Adv. Mater. 31 (2019), 1806803.
[17] Y. Chen, L. Wang, J. Shi, Nano Today 11 (2016) 292–308.
[18] D. Dolmans, D. Fukumura, R.K. Jain, Nat. Rev. Cancer 3 (2003) 380–387.
[19] V. Ntziachristos, J. Ripoll, L.H.V. Wang, R. Weissleder, Nat. Biotechnol. 23 (2005) 313–320.
[20] S.K. Maji, S. Sreejith, J. Joseph, M. Lin, T. He, Y. Tong, H. Sun, S.W.-K. Yu, Y. Zhao, Adv. Mater. 26 (2014) 5633–5638.
[21] F.T. Dastous, F.S. Foster, Ultrasound Med. Biol. 12 (1986) 795–808.
[22] S.L. Jacques, Phys. Med. Biol. 58 (2013) R37–R61.
[23] A. Zlitni, S.S. Gambhir, Curr. Opin. Chem. Biol. 45 (2018) 113–120.
[24] L. Abou-Elkacem, S.V. Bachawal, J.K. Willmann, Eur. J. Radiol. 84 (2015) 1685–1693.
[25] T. van Rooij, V. Daeichin, I. Skachkov, N. de Jong, K. Kooiman, Int. J. Hyperthermia 31 (2015) 90–106.
[26] K. Wei, A.R. Jayaweera, S. Firoozan, A. Linka, D.M. Skyba, S. Kaul, Circulation 97 (1998) 473–483.
[27] J.R. Lindner, Nat. Rev. Drug Discov. 3 (2004) 527–532.
[28] E.G. Schutt, D.H. Klein, R.M. Mattrey, J.G. Riess, Angew. Chem. Int. Ed. 42 (2003) 3218–3235.
[29] S. Hernot, A.L. Klibanov, Adv. Drug Deliv. Rev. 60 (2008) 1153–1166.
[30] E.C. Unger, T. Porter, W. Culp, R. Labell, T. Matsunaga, R. Zutshi, Adv. Drug Deliv. Rev. 56 (2004) 1291–1314.
[31] B.E. Oeffinger, M.A. Wheatley, Ultrasonics 42 (2004) 343–347.
[32] N. Chang, D. Qin, P. Wu, S. Xu, S. Wang, M. Wan, Ultrason. Sonochem. 53 (2019) 59–67.
[33] R. Teranishi, T. Matsuda, E. Yuba, K. Kono, A. Harada,Macromol. Biosci. 19 (2019), e1800365.
[34] Y. He, J. Wan, Y. Yang, P. Yuan, C. Yang, Z. Wang, L. Zhang,Adv. Healthc. Mater. (2019), e1801254.
[35] M. Lafond, S. Yoshizawa, S.I. Umemura, J. Ultrasound Med. 38 (2019) 567–580.
[36] Y. Sun, H.P. Wang, P. Wang, K. Zhang, X.R. Geng, Q.H. Liu, X.B. Wang, Biomater. Sci. 7 (2019) 985–994.
[37] A.Q. Ma, H.Q. Chen, Y.H. Cui, Z.Y. Luo, R.J. Liang, Z.H. Wu, Z. Chen, T. Yin, J. Ni, M.B. Zheng, L.T. Cai,Small 15 (2019), 1804028.
[38] K.Y. He, H.T. Ran, Z.Z. Su, Z.G. Wang, M.P. Li, L. Hao, Int. J. Nanomed. 14 (2019) 519–529.
[39] N. Chang, S.K. Lu, D. Qin, T.Q. Xu, M. Han, S.P. Wang, M.X. Wan, Ultrason. Sonochem. 45 (2018) 57–64.
[40] J.R. McLaughlan, D.M.J. Cowell, S. Freear,Phys. Med. Biol. 63 (2018), 015004.
[41] H. Han, H. Lee, K. Kim, H. Kim, J. Control. Release 266 (2017) 75–86.
[42] X.Q. Qian, X.X. Han, Y. Chen, Biomaterials 142 (2017) 13–30.
[43] A. Yildirim, R. Chattaraj, N.T. Blum, D. Shi, K. Kumar, A.P. Goodwin,Adv. Healthc. Mater. 6 (2017), 1700514.
[44] Y. Zhou, X.X. Han, X.X. Jing, Y. Chen,Adv. Healthc. Mater. 6 (2017), 1700646.
[45] N.T. Blum, A. Yildirim, R. Chattaraj, A.P. Goodwin, Theranostics 7 (2017) 694–702.
[46] H. Tang, Y. Zheng, Y. Chen,Adv. Mater. 29 (2017), 1604105.
[47] X. Wang, W. Wang, L. Yu, Y. Tang, J. Cao, Y. Chen, J. Mater. Chem. B 5 (2017) 4579–4586.
[48] X. Han, J. Huang, X. Jing, D. Yang, H. Lin, Z. Wang, P. Li, Y. Chen, ACS Nano 12 (2018) 4545–4555.
[49] C. Dai, S. Zhang, Z. Liu, R. Wu, Y. Chen, ACS Nano 11 (2017) 9467–9480.
[50] Y. Chen, Y. Gao, H.R. Chen, D.P. Zeng, Y.P. Li, Y.Y. Zheng, F.Q. Li, X.F. Ji, X. Wang, F. Chen, Q.J. He, L.L. Zhang, J.L. Shi, Adv. Funct. Mater. 22 (2012) 1586–1597.

[51] Y. Chen, H. Chen, J. Shi, Adv. Healthc. Mater. 4 (2015) 158–165.
[52] X. Wang, H.R. Chen, Y. Chen, M. Ma, K. Zhang, F.Q. Li, Y.Y. Zheng, D.P. Zeng, Q. Wang, J.L. Shi, Adv. Mater. 24 (2012) 785–791.
[53] P. Li, Y. Zheng, H. Ran, J. Tan, Y. Lin, Q. Zhang, J. Ren, Z. Wang, J. Control. Release 162 (2012) 349–354.
[54] Y. Chen, Q. Meng, M. Wu, S. Wang, P. Xu, H. Chen, Y. Li, L. Zhang, L. Wang, J. Shi, J. Am. Chem. Soc. 136 (2014) 16326–16334.
[55] M. Xu, H. Zhou, Y. Liu, J. Sun, W. Xie, P. Zhao, J. Liu, ACS Appl. Mater. Interfaces 10 (2018) 32965–32980.
[56] P. Huang, X. Qian, Y. Chen, L. Yu, H. Lin, L. Wang, Y. Zhu, J. Shi, J. Am. Chem. Soc. 139 (2017) 1275–1284.
[57] K. Ninomiya, A. Fukuda, C. Ogino, N. Shimizu, Ultrason. Sonochem. 21 (2014) 1624–1628.
[58] P. Zhu, Y. Chen, J. Shi, ACS Nano 12 (2018) 3780–3795.
[59] H. Yang, W. Cai, L. Xu, X. Lv, Y. Qiao, P. Li, H. Wu, Y. Yang, L. Zhang, Y. Duan, Biomaterials 37 (2015) 279–288.
[60] H. Zhang, J. Chen, X. Zhu, Y. Ren, F. Cao, L. Zhu, L. Hou, H. Zhang, Z. Zhang, J. Mater. Chem. B 6 (2018) 6108–6121.
[61] Q. Xia, Y. Zhang, Z. Li, X. Hou, N. Feng, Acta Pharm. Sin. B 9 (2019) 675–689.
[62] S. Sreejith, J. Joseph, M. Lin, N.V. Menon, P. Borah, H.J. Ng, Y.X. Loong, Y. Kang, S.W.K. Yu, Y. Zhao, ACS Nano 9 (2015) 5695–5704.
[63] P. Anees, J. Joseph, S. Sreejith, N.V. Menon, Y. Kang, S.W.-K. Yu, A. Ajayaghosh, Y. Zhao, Chem. Sci. 7 (2016) 4110–4116.
[64] C. Dai, Y. Chen, X. Jing, L. Xiang, D. Yang, H. Lin, Z. Liu, X. Han, R. Wu, ACS Nano 11 (2017) 12696–12712.
[65] H. Lin, Y. Chen, J. Shi,Adv. Sci. 5 (2018), 1800518.
[66] O. Couture, P.D. Bevan, E. Cherin, K. Cheung, P.N. Burns, F.S. Foster, Ultrasound Med. Biol. 32 (2006) 1247–1255.
[67] S.K. Hobbs, W.L. Monsky, F. Yuan, W.G. Roberts, L. Griffith, V.P. Torchilin, R.K. Jain, Proc. Natl. Acad. Sci. U. S. A. 95 (1998) 4607–4612.
[68] I. Brigger, C. Dubernet, P. Couvreur, Adv. Drug Deliv. Rev. 54 (2002) 631–651.
[69] E. Huynh, B.Y.C. Leung, B.L. Helfield, M. Shakiba, J.-A. Gandier, C.S. Jin, E.R. Master, B.C. Wilson, D.E. Goertz, G. Zheng, Nat. Nanotechnol. 10 (2015) 325–332.
[70] S. Gao, G.H. Wang, Z.N. Qin, X.Y. Wang, G.Q. Zhao, Q.J. Ma, L. Zhu, Biomaterials 112 (2017) 324–335.
[71] D.H. Hu, Z.W. Chen, Z.H. Sheng, D.Y. Gao, F. Yan, T. Ma, H.R. Zheng, M. Hong, Nanoscale 10 (2018) 17283–17292.
[72] Y. Wang, G.Q. Sui, D.K. Teng, Q.M.H. Wang, J. Qu, L.Y. Zhu, H.T. Ran, Z.G. Wang, C.X. Jin, H. Wang, Biomater. Sci. 7 (2019) 196–210.
[73] Z.L. Yang, W. Tian, Q. Wang, Y. Zhao, Y.L. Zhang, Y. Tian, Y.X. Tang, S.J. Wang, Y. Liu, Q.Q. Ni, G.M. Lu, Z.G. Teng, L.J. Zhang,Adv. Sci. 5 (2018), 1700847.
[74] M. Yu, X.L. Xu, Y.J. Cai, L.Y. Zou, X.T. Shuai, Biomaterials 175 (2018) 61–71.
[75] L.E. Andrews, M.H. Chan, R.S. Liu,Nanotechnology 30 (2019), 182001.
[76] L.D. Yu, P. Hu, Y. Chen,Adv. Mater. 30 (2018), 1801964.
[77] K. Wilson, K. Homan, S. Emelianov, Nat. Commun. 3 (2012) 618.
[78] G.P. Luke, A.S. Hannah, S.Y. Emelianov, Nano Lett. 16 (2016) 2556–2559.
[79] G. Yu, J. Yang, X. Fu, Z. Wang, L. Shao, Z. Mao, Y. Liu, Z. Yang, F. Zhang, W. Fan, J. Song, Z. Zhou, C. Gao, F. Huang, X. Chen, Mater. Horiz. 5 (2018) 429–435.
[80] Y. Liu, F. Yang, C. Yuan, M. Li, T. Wang, B. Chen, J. Jin, P. Zhao, J. Tong, S. Luo, N. Gu, ACS Nano 11 (2017) 1509–1519.
[81] E. Kang, H.S. Min, J. Lee, M.H. Han, H.J. Ahn, I.C. Yoon, K. Choi, K. Kim, K. Park, I.C. Kwon, Angew. Chem. Int. Ed. 49 (2010) 524–528.
[82] Y.J. Lv, Y. Cao, P. Li, J.X. Liu, H.L. Chen, W.J. Hu, L.K. Zhang,Adv. Healthc. Mater. 6 (2017), 1700354.
[83] J.V. Jokerst, C. Khademi, S.S. Gambhir,Sci. Transl. Med. 5 (2013), 177ra35.
[84] A. Liberman, Z. Wu, C.V. Barback, R. Viveros, S.L. Blair, L.G. Ellies, D.R. Vera, R.F. Mattrey, A.C. Kummel, W.C. Trogler, ACS Nano 7 (2013) 6367–6377.
[85] L. An, H. Hu, J. Du, J. Wei, L. Wang, H. Yang, D.M. Wu, H.L. Shi, F.H. Li, S.P. Yang, Biomaterials 35 (2014) 5381–5392.
[86] N.H. Tsao, E.A.H. Hall, Langmuir 32 (2016) 6534–6543.
[87] A. Liberman, J. Wang, N. Lu, R.D. Viveros, C.A. Allen, R.F. Mattrey, S.L. Blair, W.C. Trogler, M.J. Kim, A.C. Kummel, Adv. Funct. Mater. 25 (2015) 4049–4057.
[88] A. Yildirim, R. Chattaraj, N.T. Blum, A.P. Goodwin, Chem. Mater. 28 (2016) 5962–5972.
[89] K. Zhang, H. Chen, X. Guo, D. Zhang, Y. Zheng, H. Zheng, J. Shi, Sci. Rep. 5 (2015) 8766.
[90] Q. Jin, C.Y. Lin, S.T. Kang, Y.C. Chang, H. Zheng, C.M. Yang, C.K. Yeh, Ultrason. Sonochem. 36 (2017) 262–269.
[91] A. Yildirim, R. Chattaraj, N.T. Blum, G.M. Goldscheitter, A.P. Goodwin, Adv. Healthc. Mater. 5 (2016) 1290–1298.
[92] F. Chen, M. Ma, J. Wang, F. Wang, S.-X. Chern, E.R. Zhao, A. Jhunjhunwala, S. Darmadi, H. Chen, J.V. Jokerst, Nanoscale 9 (2017) 402–411.
[93] M.A. Malvindi, A. Greco, F. Conversano, A. Figuerola, M. Corti, M. Bonora, A. Lascialfari, H.A. Doumari, M. Moscardini, R. Cingolani, G. Gigli, S. Casciaro, T. Pellegrino, A. Ragusa, Adv. Funct. Mater. 21 (2011) 2548–2555.
[94] Y. Chen, H. Chen, S. Zhang, F. Chen, S. Sun, Q. He, M. Ma, X. Wang, H. Wu, L. Zhang, L. Zhang, J. Shi, Biomaterials 33 (2012) 2388–2398.
[95] M.G. Shapiro, P.W. Goodwill, A. Neogy, M. Yin, F.S. Foster, D.V. Schaffer, S.M. Conolly, Nat. Nanotechnol. 9 (2014) 311–316.
[96] R.W. Bourdeau, A. Lee-Gosselin, A. Lakshmanan, A. Farhadi, S.R. Kumar, S.P. Nety, M.G. Shapiro, Nature 553 (2018) 86–90.
[97] D.J. Park, K.H. Min, H.J. Lee, K. Kim, I.C. Kwon, S.Y. Jeong, S.C. Lee, J. Mater. Chem. B 4 (2016) 1219–1227.
[98] K.H. Min, H.S. Min, H.J. Lee, D.J. Park, J.Y. Yhee, K. Kim, I.C. Kwon, S.Y. Jeong, O.F. Silvestre, X. Chen, Y.S. Hwang, E.C. Kim, S.C. Lee, ACS Nano 9 (2015) 134–145.
[99] K.J. Chen, H.F. Liang, H.L. Chen, Y. Wang, P.Y. Cheng, H.L. Liu, Y. Xia, H.W. Sung, ACS Nano 7 (2013) 438–446.
[100] M. Yu, X. Xu, Y. Cai, L. Zou, X. Shuai, Biomaterials 175 (2018) 61–71.
[101] Y. Zhou, Z. Wang, Y. Chen, H. Shen, Z. Luo, A. Li, Q. Wang, H. Ran, P. Li, W. Song, Z. Yang, H. Chen, Z. Wang, G. Lu, Y. Zheng, Adv. Mater. 25 (2013) 4123–4130.
[102] K. Zhang, H. Chen, F. Li, Q. Wang, S. Zheng, H. Xu, M. Ma, X. Jia, Y. Chen, J. Mou, X. Wang, J. Shi, Biomaterials 35 (2014) 5875–5885.
[103] H. Tang, Y. Guo, L. Peng, H. Fang, Z. Wang, Y. Zheng, H. Ran, Y. Chen, ACS Appl. Mater. Interfaces 10 (2018) 15428–15441.
[104] K. Zhang, H. Xu, H. Chen, X. Jia, S. Zheng, X. Cai, R. Wang, J. Mou, Y. Zheng, J. Shi, Theranostics 5 (2015) 1291.
[105] A. Gnanaskandan, C.T. Hsiao, G. Chahine, Ultrasound Med. Biol. 45 (2019) 1743–1761.
[106] J.Q. Wang, L. Zhang, J. Zhang, Y.H. Ma, W. Yang, L.F. Ran, C.B. Jin, D.D. Dobromir, Z. Hui, Z. Kun, J. Ultrasound Med. 37 (2018) 2811–2819.
[107] V.G. Deepagan, D.G. You, W. Um, H. Ko, S. Kwon, K.Y. Choi, G.R. Yi, J.Y. Lee, D.S. Lee, K. Kim, I.C. Kwon, J.H. Park, Nano Lett. 16 (2016) 6257–6264.
[108] A. Jozefczak, K. Kaczmarek, T. Hornowski, M. Kubovcikova, Z. Rozynek, M. Timko, A. Skumiel, Appl. Phys. Lett. 108 (2016).
[109] X. Qian, Y. Zheng, Y. Chen, Adv. Mater. 28 (2016) 8097–8129.
[110] M. Trendowski, Cancer Metastasis Rev. 33 (2014) 143–160.
[111] D. Costley, C. Mc Ewan, C. Fowley, A.P. McHale, J. Atchison, N. Nomikou, J.F. Callan, Int. J. Hyperthermia 31 (2015) 107–117.
[112] K. Tachibana, L.B. Feril, Y. Ikeda-Dantsuji, Ultrasonics 48 (2008) 253–259.
[113] Y. Harada, K. Ogawa, Y. Irie, H. Endo, L.B. Feril Jr., T. Uemura, K. Tachibana, J. Control. Release 149 (2011) 190–195.
[114] D.G. You, V.G. Deepagan, W. Um, S. Jeon, S. Son, H. Chang, H.I. Yoon, Y.W. Cho, M. Swierczewska, S. Lee, M.G. Pomper, I.C. Kwon, K. Kim, J.H. Park, Sci. Rep. 6 (2016) 23200.
[115] K. Ninomiya, K. Noda, C. Ogino, S.-i. Kuroda, N. Shimizu, Ultrason. Sonochem. 21 (2014) 289–294.
[116] K. Ninomiya, C. Ogino, S. Oshima, S. Sonoke, S.-i. Kuroda, N. Shimizu, Ultrason. Sonochem. 19 (2012) 607–614.
[117] P. Yuan, D. Song,Nanotechnology 29 (2018), 125101.
[118] F. Gao, G. He, H. Yin, J. Chen, Y. Liu, C. Lan, S. Zhang, B. Yang, Nanoscale 11 (2019) 2374–2384.
[119] Q. Feng, Y. Li, X. Yang, W. Zhang, Y. Hao, H. Zhang, L. Hou, Z. Zhang, J. Control. Release 275 (2018) 192–200.
[120] F. Gong, L. Cheng, N. Yang, O. Betzer, L. Feng, Q. Zhou, Y. Li, R. Chen, R. Popovtzer, Z. Liu,Adv. Mater. 31 (2019), 1900730.
[121] X. Pan, L. Bai, H. Wang, Q. Wu, H. Wang, S. Liu, B. Xu, X. Shi, H. Liu,Adv. Mater. 30 (2018), 1800180.
[122] B. Wang, J. An, H. Zhang, S. Zhang, H. Zhang, L. Wang, H. Zhang, Z. Zhang,Small 14 (2018), 1801372.
[123] W. Yue, L. Chen, L. Yu, B. Zhou, H. Yin, W. Ren, C. Liu, L. Guo, Y. Zhang, L. Sun, K. Zhang, H. Xu, Y. Chen, Nat. Commun. 10 (2019) 2025.
[124] F. Bosca, P.A. Bielecki, A.A. Exner, A. Barge, Bioconjug. Chem. 29 (2018) 234–240.
[125] Z. Deng, Y. Xiao, M. Pan, F. Li, W. Duan, L. Meng, X. Liu, F. Yan, H. Zheng, J. Control. Release 243 (2016) 333–341.
[126] Z. Wang, Q. He, W. Zhao, J. Luo, W. Gao, J. Control. Release 264 (2017) 66–75.
[127] B. Kang, M.B. Zheng, P. Song, A.P. Chen, J.W. Wei, J.J. Xu, Y. Shi, H.Y. Chen,Small 13 (2017), 1604228.
[128] P. Yang, D. Li, S. Jin, J. Ding, J. Guo, W. Shi, C. Wang, Biomaterials 35 (2014) 2079–2088.
[129] T.S. Anirudhan, A.S. Nair, J. Mater. Chem. B 6 (2018) 428–439.
[130] X. Wang, F. Yan, X. Liu, P. Wang, S. Shao, Y. Sun, Z. Sheng, Q. Liu, J.F. Lovell, H. Zheng, J. Control. Release 286 (2018) 358–368.
[131] J. Di, J. Yu, Q. Wang, S. Yao, D. Suo, Y. Ye, M. Pless, Y. Zhu, Y. Jing, Z. Gu, Nano Res. 10 (2017) 1393–1402.
[132] Z.K. Jin, Y.Y. Wen, Y.X. Hu, W.W. Chen, X.F. Zheng, W.S. Guo, T.F. Wang, Z.Y. Qian, B.L. Su, Q.J. He, Nanoscale 9 (2017) 3637–3645.
[133] X. Song, L. Feng, C. Liang, K. Yang, Z. Liu, Nano Lett. 16 (2016) 6145–6153.
[134] R.J.E. van den Bijgaart, D.C. Eikelenboom, M. Hoogenboom, J.J. Futterer, M.H. den Brok, G.J. Adema, Cancer Immunol. Immunother. 66 (2017) 247–258.
[135] K. Hynynen, N. McDannold, N.A. Sheikov, F.A. Jolesz, N. Vykhodtseva, Neuroimage 24 (2005) 12–20.
[136] K. Donaldson, C.A. Poland, Curr. Opin. Biotechnol. 24 (2013) 724–734.
[137] C. Buzea, I.I. Pacheco, K. Robbie, Biointerphases 2 (2007) MR17.
[138] S. Sharifi, S. Behzadi, S. Laurent, M.L. Forrest, P. Stroeve, M. Mahmoudi, Chem. Soc. Rev. 41 (2012) 2323–2343.
[139] H. Arami, A. Khandhar, D. Liggitt, K.M. Krishnan, Chem. Soc. Rev. 44 (2015) 8576–8607.
[140] A. Gnach, T. Lipinski, A. Bednarkiewicz, J. Rybka, J.A. Capobianco, Chem. Soc. Rev. 44 (2015) 1561–1584.
[141] S.J. Soenen, P. Rivera-Gil, J.M. Montenegro, W.J. Parak, S.C. De Smedt, K. Braeckmans, Nano Today 6 (2011) 446–465.
[142] C.J. Murphy, A.M. Gole, J.W. Stone, P.N. Sisco, A.M. Alkilany, E.C. Goldsmith, S.C. Baxter, Acc. Chem. Res. 41 (2008) 1721–1730.
[143] K. Hynynen, N. Mcdannold, N. Vykhodtseva, F.A. Jolesz, Radiology 220 (2001) 640–646.

[144] L.H. Li, H.M. Yi, Y.H. Wei, H.C. Yin, C.P. Chun, W.J. Shin, T.I. Chou, W.J. Jie, Y.T. Chen, C.P. Yuan, Proc. Natl. Acad. Sci. U. S. A. 107 (2010) 15205–15210.
[145] K. Manabu, M.D. Nathan, F.A. Jolesz, H. Kullervo, Proc. Natl. Acad. Sci. U. S. A. 103 (2006) 11719–11723.
[146] J.L. Paris, C. Mannaris, M. Victoria Cabanas, R. Carlisle, M. Manzano, M. Vallet-Regi, C.C. Coussios, Chem. Eng. J. 340 (2018) 2–8.
[147] S. Wilhelm, A.J. Tavares, Q. Dai, S. Ohta, J. Audet, H.F. Dvorak, W.C.W. Chan, Nat. Rev. Mater. 1 (2016) 16014.
[148] P.Y. Wu, Y.L. Jia, F. Qu, Y. Sun, P. Wang, K. Zhang, C.S. Xu, Q.H. Liu, X.B. Wang, ACS Appl. Mater. Inter. 9 (2017) 25706–25716.
[149] H. Lee, J. Han, H. Shin, H. Han, K. Na, H. Kim, J. Control. Release 283 (2018) 190–199.
[150] R. Zhao, X. Liang, B. Zhao, M. Chen, R. Liu, S. Sun, X. Yue, S. Wang, Biomaterials 173 (2018) 58–70.
[151] W.H. Liao, M.Y. Hsiao, C.W. Lo, H.S. Yang, M.K. Sun, F.H. Lin, Y. Chang, W.S. Chen, Ultrason. Sonochem. 36 (2017) 70–77.
[152] J.L. Paris, P. de la Torre, M. Victoria Cabanas, M. Manzano, A.I. Flores, M. Vallet-Regi, Acta Biomater. 83 (2019) 372–378.
[153] J.Y. Lee, C. Crake, B. Teo, D. Carugo, M. de Saint Victor, A. Seth, E. Stride,Adv. Healthc. Mater. 6 (2017), 1601246.
[154] T. Lammers, P. Koczera, S. Fokong, F. Gremse, J. Ehling, M. Vogt, A. Pich, G. Storm, M. van Zandvoort, F. Kiessling, Adv. Funct. Mater. 25 (2015) 36–43.
[155] M. Wu, W. Chen, Y. Chen, H. Zhang, C. Liu, Z. Deng, Z. Sheng, J. Chen, X. Liu, F. Yan,Adv. Sci. 5 (2018), 1700474.
[156] C.Y. Lin, H.Y. Hsieh, W.G. Pitt, C.Y. Huang, I.C. Tseng, C.K. Yeh, K.C. Wei, H.L. Liu, J. Control. Release 212 (2015) 1–9.
[157] N. Vykhodtseva, N. McDannold, K. Hynynen, Ultrasonics 48 (2008) 279–296.
[158] R.D. Airan, R.A. Meyer, N.P. Ellens, K.R. Rhodes, K. Farahani, M.G. Pomper, S.D. Kadam, J.J. Green, Nano Lett. 17 (2017) 652–659.
[159] J.L. Paris, M. Manzano, M.V. Cabañas, M. Vallet-Regí, Nanoscale 14 (2018) 6402–6408.

Prof. Xinwu Cui received his PhD degree from Goethe University Frankfurt am Main (Germany) in 2013. He pursued his research in the Caritas Krankenhaus Bad Mergentheim (Academic teaching hospital of University Wuerzburg, Germany) as a Postdoc fellow in 2014 and as a senior researcher in 2015. Currently he is a professor in the department of medical ultrasound in Tongji Hospital, Huazhong University of Science and Technology. He is one of the authors of EFSUMB (European Federation of Societies on Ultrasound in Medicine and Biology) European course books and EFSUMB recommendations and guidelines on interventional ultrasound. He has published more than 90 scientific papers in ultrasound biomedicine.

Miss Xiaoxia Han received her Bachelor and Master degree at Chongqing Medical University (CQMU). She is currently a resident in Department of Medical Ultrasound, Shanghai General Hospital, Shanghai Jiaotong University School of Medicine. Her research interests include the design, synthesis and biomedical applications of polymers, lipids and organic-inorganic hybrid photoacoustic contrast agents for multimodal imaging and ultrasound-mediated drug delivery.

Dr. Luodan Yu received her Bachelor degree at Shijiazhuang Tiedao University in 2013 and PhD degree at Shanghai Institute of Ceramics, Chinese Academy of Sciences (SICCAS) in 2018. She is currently the research associate in SICCAS. Her research includes the design and synthesis of functional nanoplatforms for versatile biomedical applications, especially on the construction of mesoporous-silica based nanosystems for molecular imaging, controllable drug release, targeted chemotherapy and biosafety/biocompatibility evaluation/optimization.

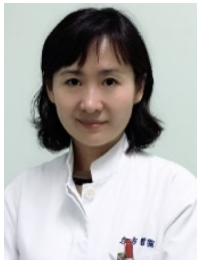

A/Prof. Bo Zhang received her PhD degree at Shanghai Jiaotong University in China. She is now a chief physician and associate professor in Shanghai East Hospital affiliated to Tongji University. Her research includes sonography diagnosis, design and synthesis of nanomaterials for molecular imaging and biological effects induced by ultrasound. She has published more than 20 scientific papers in the field of ultrasound biomedicine.

Prof. Yu Chen received his Ph.D. degree at Shanghai Institute of Ceramics, Chinese Academy of Sciences (SICCAS). He is now the full professor in SICCAS. His research includes the design, synthesis and biomedical applications of mesoporous silica/organosilica, 2D biomaterials (graphene, metal oxides, TMDCs, and MXenes) and 3D-printing bio-implants, including drug delivery, molecular imaging, nanocatalytic medicine, sonodynamic therapy, cardiac therapy, gene therapy and tissue engineering. He has published more than 150 scientific papers in nanomedicine field with a total citation of more than 11,000 times (h-index: 56). He has been awarded with the National Science Foundation for Excellent Youth Foundation, National High Level Talents Special Support Plan (Ten Thousand Plan, Young Talents) and Program of Shanghai Subject Chief Scientist.